Journal of Reliability
Science and
Engineering

PAPER • OPEN ACCESS

A new Kalman filter algorithm based on the interval process model

To cite this article: Jinyang Li *et al* 2025 *J. Reliab. Sci. Eng.* **1** 045002

View the article online for updates and enhancements.

You may also like

- Evaluating time-lagged relationships between groundwater storage and river discharge using GRACE-based data: insights from the Potomac Basin
AJ Villaruel, Alimatou Seck and Cherie Schultz
- Effect of variations of the complexity of the target variable on the assessment of Wiener–Granger causality in cardiovascular control studies
Alberto Porta, Vlasta Bari, Andrea Marchi et al.
- A dual adaptive generalized remaining life prediction method based on GP-Wiener
Hongzhi Liao, Lei Deng, Rui Xu et al.

This content was downloaded from IP address 118.123.172.215 on 17/11/2025 at 06:53

OPEN ACCESS
IOP Publishing | ISECAEP
Journal of Reliability Science and Engineering
J. Reliab. Sci. Eng. 1 (2025) 045002 (17pp)
https://doi.org/10.1088/3050-2454/ae16a8

A new Kalman filter algorithm based on the interval process model

Jinyang Li[1], Jinwu Li[1,2,*], Chengkai Shen[1], Chao Jiang[1,*] and Bingyu Ni[1]

[1] State Key Laboratory of Advanced Design and Manufacturing Technology for Vehicle, College of Mechanical and Vehicle Engineering, Hunan University, Changsha 410082, People's Republic of China
[2] School of Mechanical Engineering, Dongguan University of Technology, Dongguan 523808, People's Republic of China

E-mail: lijinwu@dgut.edu.cn and jiangc@hnu.edu.cn

Received 4 June 2025, revised 16 October 2025
Accepted for publication 20 October 2025
Published 14 November 2025

Abstract

In the traditional Kalman filter analysis, accurate noise statistics are typically required to achieve optimal estimations of parameters. However, in many practical engineering scenarios, the acquisition of sufficient samples to construct precise noise statistics is frequently constrained by limitations in testing conditions or financial considerations, which will lead to reduced precision or even divergence in the analysis results. In this paper, a novel Kalman filter algorithm is developed using an interval process model to represent noise uncertainty, only the upper and lower bounds of the noise are required during the filtering process, eliminating the need for precise probability distributions. Firstly, the uncertainty in the noise is characterized using the interval process model, and the corresponding state space equations are formulated. Secondly, a new Kalman filter algorithm is developed for both one- and multi-dimensional linear discrete systems, where the filter error variance is utilized to indicate the degree of filter estimation fluctuation. Finally, three numerical examples are investigated to validate the efficacy of the proposed algorithm.

Keywords: Kalman filter, interval process model, linear discrete system, state estimation, minimum filter error variance

1. Introduction

Filter methods are commonly employed to estimate parameters that are not directly observable or measurable. As an important technique in the filter field, the statistical filter provides the capability to implement optimal parameter estimations or predictions by using the measurement data and characteristics of signals and noises under a probability statistical framework. Wiener filter [1] and Kalman filter [2, 3] are two classical components among statistical filters. The former filters out the noises in measurement data by decomposing the power spectrum of signals and noises modeled as stationary stochastic processes. The Wiener filter is computationally prohibitive in solving the Wiener equation and can only be applied to the situation with stationary stochastic processes [4]. The Kalman filter [2, 3] establishes a time-domain recursive analysis framework to implement state estimations for both linear discrete systems and continuous systems with the Gaussian noises by minimizing the mean squared deviations of the system states, which effectively addresses the needs of a wide range of practical applications [5]. Currently, the Kalman filter is extensively applied in integrated positioning [6], fault diagnosis [7], sensor error correction [8], monitoring

* Authors to whom any correspondence should be addressed.

Original content from this work may be used under the terms of the Creative Commons Attribution 4.0 licence. Any further distribution of this work must maintain attribution to the author(s) and the title of the work, journal citation and DOI.

© 2025 The Author(s). Published by IOP Publishing Ltd on behalf of the Institute of Systems Engineering, China Academy of Engineering Physics

of damaging structures [9], lifetime prediction [10], detecting and locating [11], model predictive [12], system state estimation [13], system identification [14], remaining useful life prediction [15], etc.

In the implementation of the standard Kalman filter algorithm, employing inaccurate noise statistics may lead to insufficient accuracy of state estimation, divergence or even loss of tracking, thereby limiting the effectiveness of the algorithm in practical application [16]. To avoid excessive errors, various adaptive Kalman filter methods have been developed. These methods enhance the accuracy of final estimation and suppress the scattering by estimating and adjusting unknown noise statistical parameters, which mainly include the variational Bayesian method [17, 18], maximum likelihood method [19], covariance sampling method [20], Sage–Husa method [21], Fuzzy method [22], neural network method [23], iterative estimation method [24], information series method [25] and adaptive noise factor method [26]. However, there remain some issues for enhancing estimation accuracy and suppressing divergence [27, 28]. For example, the ability to suppress the filter divergence and estimate noise covariance would be limited when only the variance of one noise is unknown in the Sage–Husa adaptive filtering [29], and it can be poor effectiveness owing to the complexity of calculating the posterior distribution the variational Bayesian adaptive filtering [30]. The adaptive Kalman filter methods are established under the probabilistic frameworks, in which the uncertainties of both system states and external noises are described through the stochastic process model [31]. Consequently, a substantial number of experimental samples is typically needed to accurately identify the probabilistic statistical characteristics of the parameters. However, in numerous practical engineering applications, obtaining a sufficient quantity of experimental samples is difficult due to constraints in testing conditions or financial limitations, thus brings some problems in filter estimation as mentioned above. Although the adaptive filter techniques can reduce the dependence on prior statistical knowledge of noise, they cannot balance the convergence speed and estimation accuracy. Meanwhile, the accuracy of the adaptive estimation results is typically verified through simulation experiments rather than assessed by a rigorous method within the framework of existing linear minimum mean square error estimation [32, 33]. For example, in combined navigation systems, challenges such as the insufficient number of visible satellites, multi-path effects and measurement noises can lead to a mismatch in the statistical characteristics of GPS noise, which would result in poor filter effect and even serious estimation errors.

In addition, the uncertainties of system parameters are considered in some traditional Kalman filters, forming the so-called interval Kalman filters, in which the state transition matrix, control coefficient matrix and measurement gain matrix are treated as unknown but bounded constant perturbation matrices [34]. While the solution set proposed by using the upper bound of the interval matrix to be inverted may not include all the classical Kalman filter solutions an improved interval Kalman filter is therefore proposed, solving the interval matrix inversion problem with the set inversion algorithm Set Inversion Via Interval Analysis and constraint satisfaction problems [35, 36]. After that, researchers have invested significant effort in reducing both the conservatism and the high computational cost of interval Kalman filter algorithms [37]. Motivated by previous research [37], an estimation strategy that provides the optimal upper bound on the state estimation error covariance for all admissible uncertainties is developed, allowing to reduce the size of the set of all possible solutions and improve the computational efficiency of the observations with respect to the classical Kalman filtering structure [38]. By using the spectral decomposition of a symmetric matrix and optimizing the gain matrix, an improved minimum upper bound of variance interval Kalman filter is proposed, bounding the set of all possible state estimates given by the Kalman filter for any admissible parameter uncertainties [39]. Analytical bounds for optimal upper bound Kalman filter algorithm are developed by finding a uniformly optimized solution of the error estimation covariance upper bounds, reducing conservatism of the resulted estimators [40]. By extending the standard interval Kalman filtering to wireless sensor networks and incorporating global optimization techniques to search for the optimal estimation interval, a novel interval Kalman filtering algorithm is proposed, achieving higher accuracy and exhibiting less conservatism [41]. However, the interval Kalman filter mentioned above extend the classical Kalman filter technique to interval linear systems with the same statistical assumptions on noise, requiring a large number of samples to construct the probability distribution.

In this paper, therefore, a novel Kalman filter algorithm is proposed, integrating the interval process model [42, 43]. Unlike traditional methods that rely on precise probability distributions, the interval process model employs interval variables to quantify the uncertainty associated with time-variant parameters at arbitrary time instances. This methodological advancement significantly mitigates the dependence on extensive sample data during the analysis process. Within the proposed algorithm, the interval process model is leveraged to systematically characterize uncertainties in system states and noise, requiring solely the boundary information of initial system states and noise to conduct the filter estimation analysis. The remainder of this paper is organized as follows: section 2 presents a concise overview of the classical Kalman filter algorithm for linear discrete-time systems. Section 3 introduces the interval process model and formulates the new Kalman filter algorithm for linear discrete systems. Section 4 validates the proposed algorithm through three numerical examples. Finally, section 5 concludes the paper with a summary of the key findings.

2. The classical Kalman filter algorithm for linear discrete systems

The Kalman filter is formulated as an autoregressive estimation framework, through which real-time system

state estimation is performed recursively. Deterministic mathematical models of the system and measurements are utilized, along with the statistical characteristics of the initial state and noises. It is a linear unbiased and error variance-minimizing stochastic optimal algorithm, in which the system states are parameterized by the residuals of the prediction estimations and measurements. The algorithm derives the recursive state estimation equations through the minimization of the system state estimation error variances.

For a linear discrete system, its state equations and measurement equations can be expressed as [44]:

$$\begin{cases} \mathbf{X}_k = \mathbf{\Phi}_{k,k-1}\mathbf{X}_{k-1} + \mathbf{\Psi}_{k,k-1}\mathbf{U}_{k-1} + \mathbf{\Gamma}_{k,k-1}\mathbf{W}_{k-1} \\ \mathbf{Z}_k = \mathbf{H}_k\mathbf{X}_k + \mathbf{V}_k \end{cases} \tag{1}$$

where $\mathbf{X}_k, k = 1, 2, \cdots$ denotes the system state vector state with a dimension of n, $\mathbf{\Phi}_{k,k-1}$ represents $n \times n$ state transition matrix of the system, $\mathbf{\Psi}_{k,k-1}$ denotes $n \times n$ control coefficient matrix, $\mathbf{U}_{k-1}$ represents control vector with a dimension of n, $\mathbf{\Gamma}_{k,k-1}$ represents $n \times n$ noise gain matrix, $\mathbf{W}_{k-1}$ denotes process noise vector with a dimension of n, $\mathbf{Z}_k$ denotes m-dimensional measurement vector ($m \leq n$), $\mathbf{H}_k$ denotes $m \times n$ measurement gain matrix, and $\mathbf{V}_k$ denotes measurement noise vector with a dimension of m.

Assume that the process noise vector $\mathbf{W}_k$ and the measurement noise vector $\mathbf{V}_k$ are uncorrelated Gaussian white noise vectors with zero mean, namely:

$$\begin{cases} E[\mathbf{W}_k] = \mathbf{0}_{n\times 1},\ E\left[\mathbf{W}_k\mathbf{W}_j^{\mathrm{T}}\right] = \mathbf{Q}_k\delta_{k,j} \\ E[\mathbf{V}_k] = \mathbf{0}_{m\times 1},\ E\left[\mathbf{V}_k\mathbf{V}_j^{\mathrm{T}}\right] = \mathbf{R}_k\delta_{k,j} \\ E\left[\mathbf{W}_k\mathbf{V}_j^{\mathrm{T}}\right] = \mathbf{0}_{n\times m} \end{cases} \tag{2}$$

where $E[\cdot]$ is the expectation operator, $\mathbf{0}_{p_1\times p_2}$ denotes a $p_1 \times p_2$ matrix whose elements are all zeroes, $\mathbf{Q}_k$ and $\mathbf{R}_k$ are the covariance matrices corresponding to process noise vector $\mathbf{W}_k$ and measurement noise vector $\mathbf{V}_k$, respectively, $\delta_{k,j}$ is the Kronecker delta:

$$\delta_{k,j} = \begin{cases} 0, & k \neq j \\ 1, & k = j \end{cases}. \tag{3}$$

An initial condition is assumed for the system as described below:

$$\begin{cases} E[\mathbf{X}_0] = \hat{\mathbf{X}}_0,\ E\left[\left(\mathbf{X}_0 - \hat{\mathbf{X}}_0\right)\left(\mathbf{X}_0 - \hat{\mathbf{X}}_0\right)^{\mathrm{T}}\right] = \mathbf{P}_0 \\ E\left[\mathbf{X}_k\mathbf{V}_j^{\mathrm{T}}\right] = \mathbf{0}_{n\times m},\ E\left[\mathbf{X}_k\mathbf{W}_j^{\mathrm{T}}\right] = \mathbf{0}_{n\times n} \end{cases} \tag{4}$$

where $\hat{\mathbf{X}}_0$ and $\mathbf{P}_0$ are the estimation vector and covariance matrix of the initial state vector $\mathbf{X}_0$, respectively. The classical Kalman filter algorithm can be presented below [45]:

Step 1: considering the filter estimation $\hat{\mathbf{X}}_{k-1}$ from the prior step k-1, a one-step prediction estimation $\hat{\mathbf{X}}_{k,k-1}$ of the state vector $\mathbf{X}_k$ can be obtained:

$$\hat{\mathbf{X}}_{k,k-1} = \mathbf{\Phi}_{k,k-1}\hat{\mathbf{X}}_{k-1} + \mathbf{\Psi}_{k,k-1}\mathbf{U}_{k-1}. \tag{5}$$

Step 2: according to the filter error covariance matrix $\mathbf{P}_{k-1}$, the process noise covariance matrix $\mathbf{Q}_k$ and the process noise gain matrix $\mathbf{\Gamma}_{k,k-1}$, the prediction error covariance matrix $\mathbf{P}_{k,k-1}$ can be computed:

$$\mathbf{P}_{k,k-1} = \mathbf{\Phi}_{k,k-1}\mathbf{P}_{k-1}\mathbf{\Phi}_{k,k-1}^{\mathrm{T}} + \mathbf{\Gamma}_{k,k-1}\mathbf{Q}_{k-1}\mathbf{\Gamma}_{k,k-1}^{\mathrm{T}}. \tag{6}$$

Step 3: calculate the Kalman gain $\mathbf{K}_k$ according to the measurement gain matrix $\mathbf{H}_k$ and the measurement noise covariance matrix $\mathbf{R}_k$:

$$\mathbf{K}_k = \mathbf{P}_{k,k-1}\mathbf{H}_k^{\mathrm{T}}\left(\mathbf{H}_k\mathbf{P}_{k,k-1}\mathbf{H}_k^{\mathrm{T}} + \mathbf{R}_k\right)^{-1}. \tag{7}$$

Step 4: according to prediction estimation $\hat{\mathbf{X}}_{k,k-1}$, Kalman gain $\mathbf{K}_k$ and the measurement vector $\mathbf{Z}_k$, the filter estimation of the state vector $\mathbf{X}_k$ can be obtained:

$$\hat{\mathbf{X}}_k = \hat{\mathbf{X}}_{k,k-1} + \mathbf{K}_k\left(\mathbf{Z}_k - \mathbf{H}_k\hat{\mathbf{X}}_{k,k-1}\right). \tag{8}$$

Step 5: calculate the updated filter error covariance matrix:

$$\mathbf{P}_k = (\mathbf{I} - \mathbf{K}_k\mathbf{H}_k)\mathbf{P}_{k,k-1}(\mathbf{I} - \mathbf{K}_k\mathbf{H}_k)^{\mathrm{T}} + \mathbf{K}_k\mathbf{R}_k\mathbf{K}_k^{\mathrm{T}}. \tag{9}$$

Equations (5)–(9) form the basic equations of Kalman filter for linear discrete systems. When $\hat{\mathbf{X}}_0$ and $\mathbf{P}_0$ are given, the filter estimation of the state vector $\mathbf{X}_k$ based on the principle of minimizing filter error variance can be calculated recursively based on the measurement vector $\mathbf{Z}_k$.

3. The proposed Kalman filter algorithm

In this paper, a novel Kalman filter algorithm for linear discrete systems is proposed based on the interval process model, enabling optimal state estimation even when experimental samples are insufficient. Firstly, the fundamentals of the interval process model are introduced, and new definitions are provided, including the cross-covariance function matrix between interval process vectors and the concept of uncorrelated interval process vectors. Secondly, the system state and noise characteristics are described using the interval process model, and the corresponding state and measurement equations are formulated. Finally, the algorithm is established by defining the midpoint of the filter estimation as the optimal state estimate and representing its fluctuation utilizing the filter error variance. The proposed Kalman filter algorithm is designed to achieve optimal state estimation by minimizing the filter error variance.

3.1. Fundamentals of interval process model [42, 43, 46]

In traditional stochastic process theory [47], an uncertain process $X(t)$ is treated as a random variable at any given time, with the correlation between variables at different time points characterized by the auto-correlation function. However, a substantial number of samples is necessitated for the stochastic process model. To mitigate this dependency, the researchers [42, 43] recently extended the conventional interval method [48–51] to the time dimension, developing the interval process

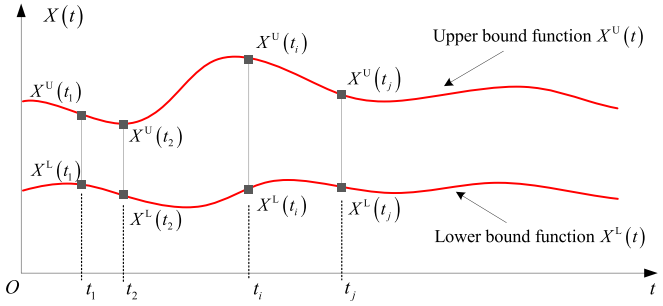


Figure 1. Interval process model [43].

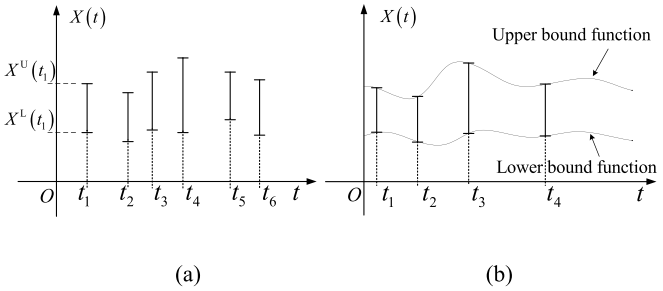


Figure 2. The classification of interval processes [42]. (a) The discrete parameter interval process; (b) the continuous parameter interval process.

model as an effective mathematical framework for addressing time-dependent or dynamic uncertainties. Unlike stochastic models, the interval process model requires only the boundary information of uncertain parameter fluctuations, which can be derived from limited samples and expert knowledge. As illustrated in figure 1, this model represents dynamic uncertainty utilizing bounded and closed intervals at any given time point.

Definition 1. For an uncertain process $\{X(t), t \in \mathbb{T}\}$, $\mathbb{T}$ is a parameter set of the parameter t, if for any given time t_i, $i = 1,2,\cdots$, $X(t_i) \in X^{I}(t_i) = \left[X^{L}(t_i), X^{U}(t_i)\right]$ is an interval variable, then the process $\{X(t), t \in \mathbb{T}\}$ is called an interval process, denoted as $\left\{X(t) \in X^{I}(t), t \in \mathbb{T}\right\}$, where superscripts I, L and U denote interval, lower bound and upper bound, respectively. For the convenience of description, the interval process can be abbreviated as $X(t) \in X^{I}(t)$ or $X^{I}(t)$ without causing ambiguity.

According to the property of parameter set $\mathbb{T}$, the interval process can be categorized into two classes in figure 2: if the parameter set $\mathbb{T}$ is a countable set (or discrete in time), this class of process is called the discrete parameter interval process, as shown in figure 2(a); if the parameter set $\mathbb{T}$ is non-countable (or continuous in time), this class of process is called the continuous parameter interval process, as shown in figure 2(b).

Definition 2. For an interval process $\left\{X(t) \in X^{I}(t), t \in \mathbb{T}\right\}$ with the upper bound function $X^{U}(t)$ and the lower bound function $X^{L}(t)$, its middle point function $M_{X^{I}}(t)$, radius function $R_{X^{I}}(t)$ and variance function $D_{X^{I}}(t)$ are, respectively, defined as:

$$M_{X^{I}}(t) = M[X(t)] = X^{m}(t) = \frac{X^{L}(t) + X^{U}(t)}{2} \tag{10}$$

$$R_{X^{I}}(t) = R[X(t)] = X^{r}(t) = \frac{X^{U}(t) - X^{L}(t)}{2} \tag{11}$$

$$D_{X^{I}}(t) = D[X(t)] = (X^{r}(t))^{2} = \left(\frac{X^{U}(t) - X^{L}(t)}{2}\right)^{2}. \tag{12}$$

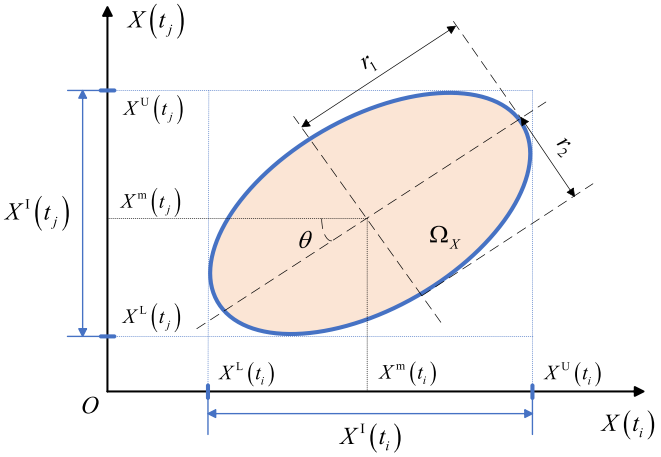


Figure 3. Interval model considering correlation [42].

In many situations, the state of a time-variant parameter at a certain time point will have a certain degree of influence or even a decisive effect on the state of the next time point or next stage, which is called time correlation in the interval process model and can be quantified using the auto-covariance function. In order to characterize the correlation degree between the interval process $X^{I}(t)$ at any two time points t_i and t_j, the joint uncertainty domain is described through an ellipse, as shown in figure 3. For interval variables $X(t_i) \in X^{I}(t_i) = \left[X^{L}(t_i), X^{U}(t_i)\right]$ and $X(t_j) \in X^{I}(t_j) = \left[X^{L}(t_j), X^{U}(t_j)\right]$, the covariance function $\mathrm{Cov}(X(t_i), X(t_j))$ is defined as:

$$\mathrm{Cov}(X(t_i), X(t_j)) = \sin(\theta)\cos(\theta)\left(r_1^2 - r_2^2\right) \tag{13}$$

where θ is the angle between the long axis and the horizontal coordinate axis, called rotation angle, r_1 and r_2 are the half lengths of the major axis and the minor axis of the ellipse, respectively, as shown in figure 3.

Definition 3. For an interval process $\left\{X(t) \in X^{I}(t), t \in \mathbb{T}\right\}$, the auto-covariance function $\mathrm{Cov}_{X^{I}X^{I}}(t_i, t_j)$ and the auto-correlation coefficient function $\rho_{X^{I}X^{I}}(t_i, t_j)$ at any two time points t_i and t_j are, respectively, defined as:

$$\mathrm{Cov}_{X^{I}X^{I}}(t_i, t_j) = \mathrm{Cov}(X(t_i), X(t_j)) \tag{14}$$

$$\rho_{X^{I}X^{I}}(t_i, t_j) = \frac{\mathrm{Cov}_{X^{I}X^{I}}(t_i, t_j)}{X^{r}(t_i) X^{r}(t_j)}. \tag{15}$$

Definition 4. For an interval process $\left\{X(t) \in X^{\mathrm{I}}(t),\ t \in \mathbb{T}\right\}$, if its auto-covariance function satisfies:

$$\mathrm{Cov}_{X^{\mathrm{I}}X^{\mathrm{I}}}(t_i, t_j) = 0, (i \neq j) \tag{16}$$

then $X^{\mathrm{I}}(t)$ is called the uncorrelated interval process.

Definition 5. The cross-covariance function of interval processes $\left\{X(t) \in X^{\mathrm{I}}(t),\ t \in \mathbb{T}\right\}$ and $\left\{Y(t) \in Y^{\mathrm{I}}(t),\ t \in \mathbb{T}\right\}$ at any two time points t_i and t_j is defined as:

$$\mathrm{Cov}_{X^{\mathrm{I}}Y^{\mathrm{I}}}(t_i, t_j) = \mathrm{Cov}\left(X(t_i), Y(t_j)\right) \tag{17}$$

Definition 6. For interval processes $\left\{X(t) \in X^{\mathrm{I}}(t),\ t \in \mathbb{T}\right\}$ and $\left\{Y(t) \in Y^{\mathrm{I}}(t),\ t \in \mathbb{T}\right\}$, if the cross-covariance function satisfies:

$$\mathrm{Cov}_{X^{\mathrm{I}}Y^{\mathrm{I}}}(t_i, t_j) = 0 \tag{18}$$

then the interval processes $X^{\mathrm{I}}(t)$ and $Y^{\mathrm{I}}(t)$ are uncorrelated.

Definition 7. Let $\left\{X_k(t) \in X_k^{\mathrm{I}}(t),\ t \in \mathbb{T}\right\}$, $k = 1, 2, \cdots, N$ be N interval processes, for each interval process $X_k^{\mathrm{I}}(t)$, the middle point function and radius function are $X_k^{\mathrm{m}}(t)$ and $X_k^{\mathrm{r}}(t)$, respectively, the auto-covariance function is $\mathrm{Cov}_{X_k^{\mathrm{I}}X_k^{\mathrm{I}}}(t_i, t_j)$, and cross-covariance function of $X_k(t)$ and $X_l(t)\,(l \neq k)$ is $\mathrm{Cov}_{X_k^{\mathrm{I}}X_l^{\mathrm{I}}}(t_i, t_j)$, then $\mathbf{X}^{\mathrm{m}}(t) = \left[X_1^{\mathrm{m}}(t), X_2^{\mathrm{m}}(t), \cdots, X_N^{\mathrm{m}}(t)\right]^T$ and $\mathbf{X}^{\mathrm{r}}(t) = \left[X_1^{\mathrm{r}}(t), X_2^{\mathrm{r}}(t), \cdots, X_N^{\mathrm{r}}(t)\right]^T$ are, respectively, called the middle point function vector and radius function vector for an N-dimensional interval process vector $\mathbf{X}(t) = \left[X_1(t), X_2(t), \cdots, X_N(t)\right]^T$, $\mathbf{Cov}_{\mathbf{X}^{\mathrm{I}}\mathbf{X}^{\mathrm{I}}}(t_i, t_j)$ is called the cross-covariance function matrix:

$$\mathbf{Cov}_{\mathbf{X}^{\mathrm{I}}\mathbf{X}^{\mathrm{I}}}(t_i, t_j) = \begin{bmatrix} \mathrm{Cov}_{X_1^{\mathrm{I}}X_1^{\mathrm{I}}}(t_i, t_j) & \mathrm{Cov}_{X_1^{\mathrm{I}}X_2^{\mathrm{I}}}(t_i, t_j) & \cdots & \mathrm{Cov}_{X_1^{\mathrm{I}}X_N^{\mathrm{I}}}(t_i, t_j) \\ \mathrm{Cov}_{X_2^{\mathrm{I}}X_1^{\mathrm{I}}}(t_i, t_j) & \mathrm{Cov}_{X_2^{\mathrm{I}}X_2^{\mathrm{I}}}(t_i, t_j) & \cdots & \mathrm{Cov}_{X_2^{\mathrm{I}}X_N^{\mathrm{I}}}(t_i, t_j) \\ \vdots & \vdots & \ddots & \vdots \\ \mathrm{Cov}_{X_N^{\mathrm{I}}X_1^{\mathrm{I}}}(t_i, t_j) & \mathrm{Cov}_{X_N^{\mathrm{I}}X_2^{\mathrm{I}}}(t_i, t_j) & \cdots & \mathrm{Cov}_{X_N^{\mathrm{I}}X_N^{\mathrm{I}}}(t_i, t_j) \end{bmatrix}. \tag{19}$$

Definition 8. For an N-dimensional interval process vector $\mathbf{X}(t) = \left[X_1(t), X_2(t), \cdots, X_N(t)\right]^T$, if any two interval processes $X_k(t)$ and $X_l(t)$ $k \neq l$ are uncorrelated, then $\mathbf{X}(t)$ is called the uncorrelated interval process vector.

Definition 9. For two interval process vectors $\mathbf{X}(t) = \left[X_1(t), X_2(t), \cdots, X_N(t)\right]^T$ and $\mathbf{Y}(t) = \left[Y_1(t), Y_2(t), \cdots, Y_M(t)\right]^T$, the cross-covariance function matrix between $\mathbf{X}(t)$ and $\mathbf{Y}(t)$ is defined as:

$$\mathbf{Cov}_{\mathbf{X}^{\mathrm{I}}\mathbf{Y}^{\mathrm{I}}}(t_i, t_j) = \begin{bmatrix} \mathrm{Cov}_{X_1^{\mathrm{I}}Y_1^{\mathrm{I}}}(t_i, t_j) & \mathrm{Cov}_{X_1^{\mathrm{I}}Y_2^{\mathrm{I}}}(t_i, t_j) & \cdots & \mathrm{Cov}_{X_1^{\mathrm{I}}Y_M^{\mathrm{I}}}(t_i, t_j) \\ \mathrm{Cov}_{X_2^{\mathrm{I}}Y_1^{\mathrm{I}}}(t_i, t_j) & \mathrm{Cov}_{X_2^{\mathrm{I}}Y_2^{\mathrm{I}}}(t_i, t_j) & \cdots & \mathrm{Cov}_{X_2^{\mathrm{I}}Y_M^{\mathrm{I}}}(t_i, t_j) \\ \vdots & \vdots & \ddots & \vdots \\ \mathrm{Cov}_{X_N^{\mathrm{I}}Y_1^{\mathrm{I}}}(t_i, t_j) & \mathrm{Cov}_{X_N^{\mathrm{I}}Y_2^{\mathrm{I}}}(t_i, t_j) & \cdots & \mathrm{Cov}_{X_N^{\mathrm{I}}Y_M^{\mathrm{I}}}(t_i, t_j) \end{bmatrix} \tag{20}$$

where $\mathrm{Cov}_{X_k^{\mathrm{I}}Y_l^{\mathrm{I}}}(t_i, t_j), k = 1, 2, \cdots, N, l = 1, 2, \cdots, M$ denotes the cross-covariance function of $X_k(t)$ and $Y_l(t)$. If $\mathbf{Cov}_{\mathbf{X}^{\mathrm{I}}\mathbf{Y}^{\mathrm{I}}}(t_i, t_j) = \mathbf{0}_{N\times M}$, then the interval process vectors $\mathbf{X}(t)$ and $\mathbf{Y}(t)$ are uncorrelated.

For two interval vectors $X = \left[X_1, X_2, \cdots, X_N\right]^T$ where $X_i \in X_i^{\mathrm{I}}, i = 1, 2, \cdots, N$ and $Y = \left[Y_1, Y_2, \cdots, Y_M\right]^T$ where $Y_i \in Y_i^{\mathrm{I}}, i = 1, 2, \cdots, M$, the cross-covariance matrix between them is defined as:

$$\mathbf{Cov}(\mathbf{X}, \mathbf{Y}) = \begin{bmatrix} \mathrm{Cov}(X_1, Y_1) & \mathrm{Cov}(X_1, Y_2) & \cdots & \mathrm{Cov}(X_1, Y_M) \\ \mathrm{Cov}(X_2, Y_1) & \mathrm{Cov}(X_2, Y_2) & \cdots & \mathrm{Cov}(X_2, Y_M) \\ \vdots & \vdots & \ddots & \vdots \\ \mathrm{Cov}(X_N, Y_1) & \mathrm{Cov}(X_N, Y_2) & \cdots & \mathrm{Cov}(X_N, Y_M) \end{bmatrix}. \tag{21}$$

If $\mathbf{Cov}(\mathbf{X}, \mathbf{Y}) = \mathbf{0}_{N\times M}$, then the interval vectors $\mathbf{X}$ and $\mathbf{Y}$ are uncorrelated.

It is worth noting that the auto-covariance function $\mathrm{Cov}_{X^{\mathrm{I}}X^{\mathrm{I}}}(t_i, t_j)$ and cross-covariance function $\mathrm{Cov}_{X_k^{\mathrm{I}}Y_l^{\mathrm{I}}}(t_i, t_j), k = 1, 2, \cdots, N, l = 1, 2, \cdots, M$ are defined to represent the correlation degree of interval variables $X(t_i)$ and $X(t_j)$, $X_k(t_i)$ and $Y_l(t_j)$, respectively. As the absolute value of the auto-covariance function or cross-covariance function increases, the corresponding ellipse will become longer and narrower, which indicates a growing correlativity of the interval variables.

3.2. Formulation of the proposed algorithm

In the classical Kalman filter theory, the stochastic process model is used to describe the uncertainty of the system state and noises in the linear discrete system. Different from the classical Kalman filter theory, here we use the interval process model to quantify the uncertainty of the system state and noises in the linear discrete system, and thus the corresponding state and measurement equations are established. In the following text, the filter algorithm is constructed for one-dimensional systems and multi-dimensional systems, respectively.

3.2.1. For one-dimensional linear systems. For a one-dimensional discrete linear system, when the process noise and the measurement noise are treated as uncorrelated interval processes $\left\{w_k \in w_k^{\mathrm{I}}, k = 1, 2, \cdots\right\}$ and $\left\{v_k \in v_k^{\mathrm{I}}, k = 1, 2, \cdots\right\}$, then its state equation and measurement equation can be expressed as:

$$\begin{cases} x_k = \varphi_{k,k-1}x_{k-1} + \psi_{k,k-1}u_{k-1} + w_{k-1} \\ z_k = h_k x_k + v_k \end{cases} \tag{22}$$

where $\varphi_{k,k-1}$ is a state transition coefficient, $\psi_{k,k-1}$ is a system control coefficient, u_{k-1} is a control variable, $z_k \in z_k^{\mathrm{I}}$ is a measurement variable, h_k is a measurement coefficient. The characteristic parameters of the process noise and measurement noise are assumed as follows:

$$\begin{cases} M[w_k] = 0,\ \mathrm{Cov}\left(w_k,\ w_j\right) = q_k\delta_{k,j} \\ M[v_k] = 0,\ \mathrm{Cov}\left(v_k,\ v_j\right) = r_k\delta_{k,j} \\ \mathrm{Cov}\left(w_k,\ v_j\right) = 0 \end{cases} \tag{23}$$

where q_k and r_k are the variance function of the process noise and the measurement noise, respectively. Assume that the initial system state $x_0 \in x_0^{\mathrm{I}}$ satisfies the following conditions:

$$\begin{cases} M[x_0] = x_0^{\mathrm{m}}, \quad D[x_0] = P_0 \\ \mathrm{Cov}(x_0, w_k) = 0, \quad \mathrm{Cov}(x_0,\ v_k) = 0 \end{cases} \tag{24}$$

where x_0^{m} and P_0 are the estimation and variance of the initial system state, respectively.

Assume that there exist measurements $z_1, z_2, \cdots, z_k$ and the optimal filter estimation $\hat{x}_{k-1}$ of x_{k-1} in the time step k, then a reasonable or ideal state prediction estimation can be expressed as:

$$\hat{x}_{k,k-1} = \varphi_{k,k-1}\hat{x}_{k-1} + \psi_{k,k-1}u_{k-1} \tag{25}$$

and the prediction estimation of the measurement variable z_k can be expressed as:

$$\hat{z}_{k,k-1} = h_k\hat{x}_{k,k-1}. \tag{26}$$

The measurement residual between z_k and $\hat{z}_{k,k-1}$ is defined as:

$$\tilde{z}_{k,k-1} = z_k - \hat{z}_{k,k-1} = z_k - h_k\hat{x}_{k,k-1}. \tag{27}$$

By using the measurement residual to correct the original state prediction estimation, the optimal filter estimation at the time step k can be expressed as:

$$\hat{x}_k = \hat{x}_{k,k-1} + g_k \times \left(z_k - h_k\hat{x}_{k,k-1}\right) \tag{28}$$

where g_k is the filter gain. The prediction error $e_{k,k-1}$ and the filter error e_k are, respectively, defined as:

$$e_{k,k-1} = x_k - \hat{x}_{k,k-1} \tag{29}$$

$$e_k = x_k - \hat{x}_k. \tag{30}$$

Substitute equations (22) and (25) into equation (29) yields:

$$e_{k,k-1} = \varphi_{k,k-1}\left(x_{k-1} - \hat{x}_{k-1}\right) + w_{k-1}. \tag{31}$$

Substitute equations (22) and (28) into equation (30) yields:

$$e_k = [1 - k_h h_k]\left(x_k - \hat{x}_{k,k-1}\right) + g_k v_k. \tag{32}$$

According to equation (31), the prediction error variance $P_{k,k-1}$ can be obtained:

$$\begin{aligned} P_{k,k-1} &= D\left[e_{k,k-1}\right] = \mathrm{Cov}\left(e_{k,k-1}, e_{k,k-1}\right) \\ &= \varphi_{k,k-1}^2\mathrm{Cov}\left(x_{k-1} - \hat{x}_{k-1}, x_{k-1} - \hat{x}_{k-1}\right) \\ &\quad +2\varphi_{k,k-1}\mathrm{Cov}\left(x_{k-1} - \hat{x}_{k-1}, w_{k-1}\right) + \mathrm{Cov}\left(w_{k-1}, w_{k-1}\right) \end{aligned} . \tag{33}$$

It can be proved that $\mathrm{Cov}\left(x_{k-1} - \hat{x}_{k-1}, w_{k-1}\right) = 0$, and equation (33) can be simplified as:

$$P_{k,k-1} = \varphi_{k,k-1}^2 P_{k-1} + q_{k-1}. \tag{34}$$

According to equation (32), the filter error variance P_k can be obtained:

$$\begin{aligned} P_k &= D[e_k] = \mathrm{Cov}(e_k, e_k) \\ &= (1 - g_k h_k)^2\mathrm{Cov}\left(x_k - \hat{x}_{k,k-1}, x_k - \hat{x}_{k,k-1}\right) \\ &\quad -2k_k(1 - g_k h_k)\mathrm{Cov}\left(x_k - \hat{x}_{k,k-1}, v_k\right) + g_k^2\mathrm{Cov}(v_k, v_k) \end{aligned} . \tag{35}$$

It can be proved that $\mathrm{Cov}\left(x_k - \hat{x}_{k,k-1}, v_k\right) = 0$, and equation (35) can be simplified as:

$$P_k = (1 - g_k h_k)^2 P_{k,k-1} + g_k^2 r_k. \tag{36}$$

To calculate the gain g_k for a minimum filter error variance, let:

$$\frac{\partial P_k}{\partial g_k} = \frac{\partial\left((1 - g_k h_k)^2 P_{k,k-1} + g_k^2 r_k\right)}{\partial g_k} = 0 \tag{37}$$

then g_k can be solved:

$$g_k = \frac{h_k P_{k,k-1}}{h_k^2 P_{k,k-1} + r_k}. \tag{38}$$

To sum up, the basic equations of the proposed Kalman filter algorithm for one-dimensional linear discrete system based on the interval process model can be established as follows:

$$\hat{x}_{k,k-1} = \varphi_{k,k-1}\hat{x}_{k-1} + \psi_{k,k-1}u_{k-1} \tag{39}$$

$$P_{k,k-1} = \varphi_{k,k-1}^2 P_{k-1} + q_{k-1} \tag{40}$$

$$g_k = \frac{h_k P_{k,k-1}}{h_k^2 P_{k,k-1} + r_k} \tag{41}$$

$$\hat{x}_k = \hat{x}_{k,k-1} + g_k\left(z_k - h_k\hat{x}_{k,k-1}\right) \tag{42}$$

$$P_k = (1 - g_k h_k)^2 P_{k,k-1} + g_k^2 r_k. \tag{43}$$

The middle point of $\hat{x}_k$ is used as the optimal state estimation at the time step k in the sense of minimum filter error variance, and P_k can reflect the degree of fluctuation.

3.2.2. For multi-dimensional linear systems. For a multi-dimensional discrete linear system, the state and measurement equations can be expressed as equation (1). Treat the process noise vector and the measurement noise vector as uncorrelated interval process vectors $\mathbf{W}_k^{\mathrm{I}}$ and $\mathbf{V}_k^{\mathrm{I}}$, respectively. Assume the characteristic parameters of $\mathbf{W}_k$ and $\mathbf{V}_k$ as follows:

$$\begin{cases} M[\mathbf{W}_k] = \mathbf{0}_{n\times 1}, \ \mathbf{Cov}_{\mathbf{W}^{\mathrm{I}}\mathbf{W}^{\mathrm{I}}}(k, j) = \mathbf{Q}_k\delta_{k,j} \\ M[\mathbf{V}_k] = \mathbf{0}_{m\times 1}, \ \mathbf{Cov}_{\mathbf{V}^{\mathrm{I}}\mathbf{V}^{\mathrm{I}}}(k, j) = \mathbf{R}_k\delta_{k,j} \\ \mathbf{Cov}_{\mathbf{W}^{\mathrm{I}}\mathbf{V}^{\mathrm{I}}}(k, j) = \mathbf{0}_{n\times m} \end{cases} \tag{44}$$

where $\mathbf{Q}_k$ and $\mathbf{R}_k$ are the covariance matrices of the process noise vector and the measurement noise vector at the time step k, respectively. Assume that the initial system state $\mathbf{X}_0$ satisfies the following conditions:

$$\begin{cases} M[\mathbf{X}_0] = \mathbf{X}_0^{\mathrm{m}}, \quad \mathbf{Cov}(\mathbf{X}_0, \mathbf{X}_0) = \mathbf{P}_0 \\ \mathbf{Cov}(\mathbf{X}_0, \mathbf{W}_k) = \mathbf{0}_{n\times n}, \ \mathbf{Cov}\left(\mathbf{X}_0,\ \mathbf{V}_j\right) = \mathbf{0}_{n\times m} \end{cases} \tag{45}$$

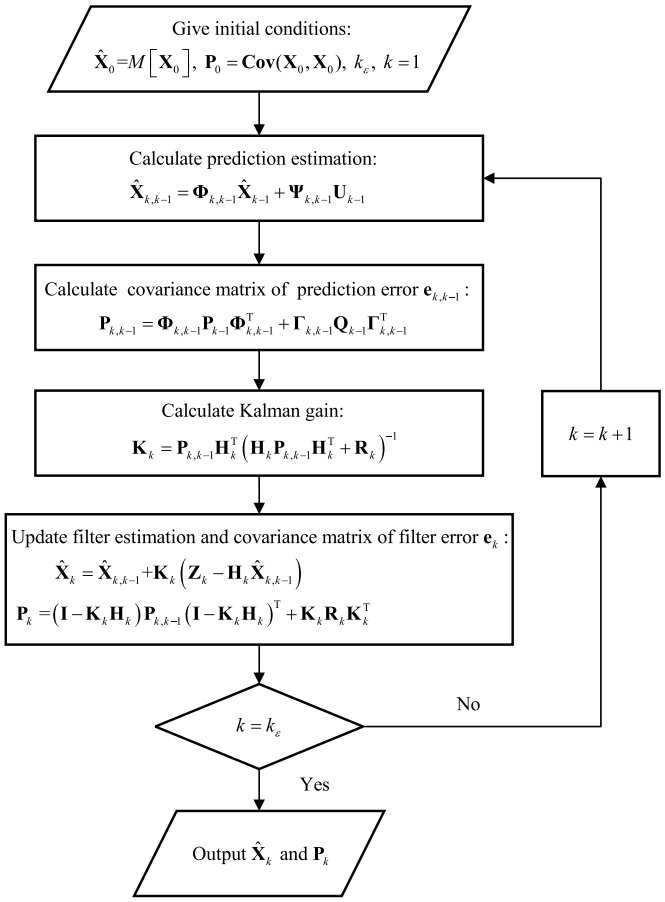


Figure 4. The flowchart of the calculation procedure for state estimation of the proposed Kalman filter algorithm.

where $\mathbf{X}_0^{\mathrm{m}}$ and $\mathbf{P}_0$ are the estimation vector and the covariance matrix of the initial system state, respectively.

Assuming that there exist the measurements $\mathbf{Z}_1,\mathbf{Z}_2,\cdots,\mathbf{Z}_k$ and the optimal filter estimation $\hat{\mathbf{X}}_{k-1}$ of $\mathbf{X}_{k-1}$ at the time step k, the basic equations of the proposed Kalman filter algorithm for the multi-dimensional linear discrete system based on the interval process model can be established as follows:

$$\hat{\mathbf{X}}_{k,k-1}=\mathbf{\Phi}_{k,k-1}\hat{\mathbf{X}}_{k-1}+\mathbf{\Psi}_{k,k-1}\mathbf{U}_{k-1} \tag{46}$$

$$\mathbf{P}_{k,k-1}=\mathbf{\Phi}_{k,k-1}\mathbf{P}_{k-1}\mathbf{\Phi}_{k,k-1}^{\mathrm{T}}+\mathbf{\Gamma}_{k,k-1}\mathbf{Q}_{k-1}\mathbf{\Gamma}_{k,k-1}^{\mathrm{T}} \tag{47}$$

$$\mathbf{K}_k=\mathbf{P}_{k,k-1}\mathbf{H}_k^{\mathrm{T}}\left(\mathbf{H}_k\mathbf{P}_{k,k-1}\mathbf{H}_k^{\mathrm{T}}+\mathbf{R}_k\right)^{-1} \tag{48}$$

$$\hat{\mathbf{X}}_k=\hat{\mathbf{X}}_{k,k-1}+\mathbf{K}_k\left(\mathbf{Z}_k-\mathbf{H}_k\hat{\mathbf{X}}_{k,k-1}\right) \tag{49}$$

$$\mathbf{P}_k=\left(\mathbf{I}-\mathbf{K}_k\mathbf{H}_k\right)\mathbf{P}_{k,k-1}\left(\mathbf{I}-\mathbf{K}_k\mathbf{H}_k\right)^{\mathrm{T}}+\mathbf{K}_k\mathbf{R}_k\mathbf{K}_k^{\mathrm{T}} \tag{50}$$

where the detailed derivation of gain matrix $\mathbf{K}_k$ is given in the Appendix. The middle point vector of $\hat{\mathbf{X}}_k$ is used as the optimal state estimation at the time step k and the diagonal elements of $\mathbf{P}_k$ can reflect the fluctuation degree for each element of $\hat{\mathbf{X}}_k$. The flowchart of the proposed Kalman filter algorithm is shown as figure 4.

The filter algorithm for one-dimensional systems and multi-dimensional systems subject to uncorrelated noises has now been formulated. When the initial estimation and the variance of system state are given, the optimal state estimation at each time step of k in the sense of the minimum filter error variance can be calculated recursively based on the measurements. The proposed algorithm avoids the use of precise probability characteristics and theoretically could greatly reduce the dependence of the whole analysis process on a large number of samples.

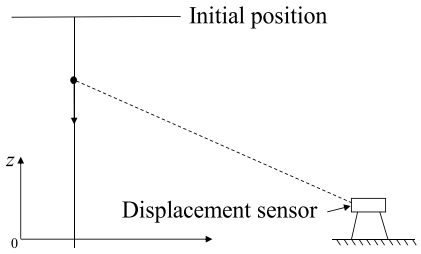


Figure 5. Schematic diagram of a free-fall moving target tracking problem.

4. Numerical examples and discussions

4.1. A free-fall moving target tracking problem

Consider a free-fall moving target tracking problem as illustrated in figure 5. The target is observed by the displacement sensor, with observation period $T_0=0.01\,\mathrm{s}$ and total observation time 10 s. In order to obtain data more accurately, the displacement and velocity of the target are needed to be estimated, especially when the sensor's measurement is disturbed by noise. Here, the distance between the target and the ground is calibrated along the z-axis which extends vertically upwards from the ground. The displacement and velocity of the target at the time step k are denoted as x_k and $\dot{x}_k$, respectively. The following state vector is defined:

$$\mathbf{X}_k=[x_k,\ \dot{x}_k]^{\mathrm{T}}. \tag{51}$$

From the kinematics knowledge [52], the state equation and measurement equation of the free-fall moving target tracking problem can be formulated as follows:

$$\begin{cases}\mathbf{X}_k=\mathbf{\Phi}\mathbf{X}_{k-1}+\mathbf{\Psi}\left(-g\right)\\ y_k=\mathbf{H}\mathbf{X}_k+v_k\end{cases} \tag{52}$$

where $\mathbf{\Phi}=\begin{bmatrix}1 & T_0\\ 0 & 1\end{bmatrix}$, $\mathbf{\Psi}=\left[0.5T_0^2,T_0\right]^{\mathrm{T}}$, $\mathbf{H}=[1,0]$, and $g=10\,\mathrm{m}\cdot\mathrm{s}^{-2}$ is the gravitational acceleration. The initial state is described by an interval vector $\mathbf{X}_0$ with the middle point vector $\mathbf{X}_0^{\mathrm{m}}=[100,\ 0]^{\mathrm{T}}$ and the covariance matrix:

$$\mathbf{P}_0=\begin{bmatrix}1 & 0\\ 0 & 1\end{bmatrix}. \tag{53}$$

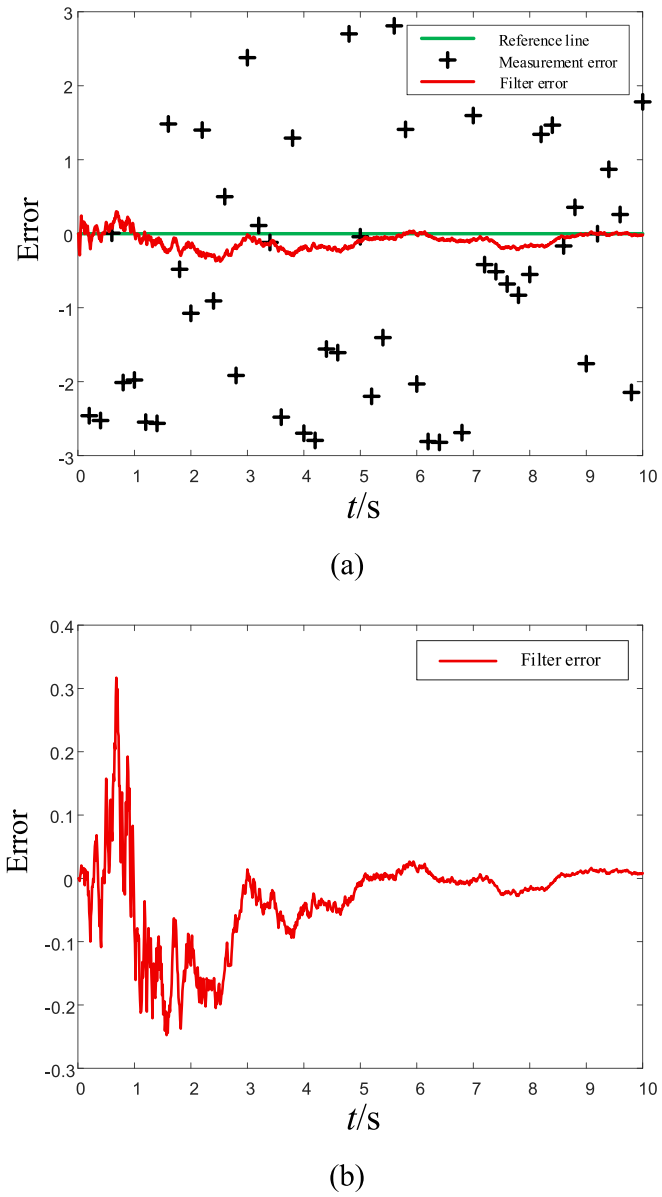


Figure 6. Filter error curves for state estimation in the free-fall moving target tracking problem using traditional algorithm. (a) Displacement; (b) velocity.

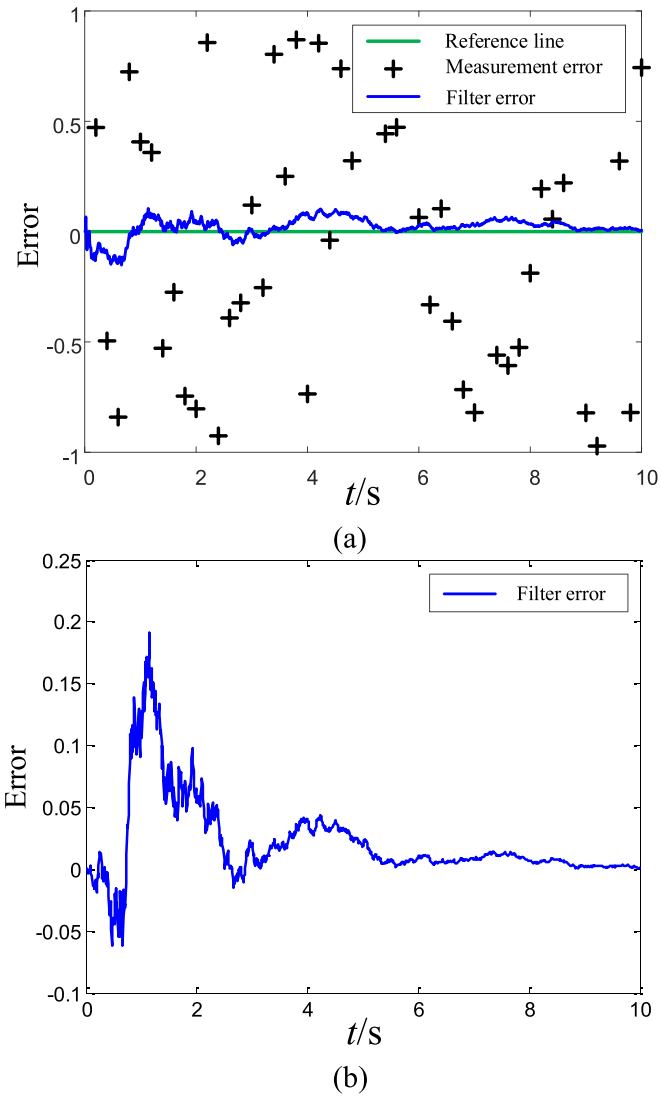


Figure 7. Filter error curves for state estimation in the free-fall moving target tracking problem using proposed algorithm. (a) Displacement; (b) velocity.

Firstly, the convergence of the proposed filter algorithm for the free-fall moving target tracking problem is investigated. The traditional Kalman filter algorithm with the uncorrelated Gaussian noise assumption is applied as a comparison for the proposed algorithm. For the traditional algorithm, the system states are represented by stochastic variables with the initial mean vector $\mu(\mathbf{X}_0) = [100,\ 0]^{\mathrm{T}}$, and the measurement noise is regarded as an uncorrelated stochastic process $\{u(k), k = 1, 2, \cdots\}$ with mean function $\mu(u(k)) = 0$ and variance function $D(u(k)) = 9$. While for the proposed algorithm the noise is treated as an uncorrelated interval process $\{v_k \in v_k^{\mathrm{I}}, k = 1, 2, \cdots\}$ with the middle point function $v_k^{\mathrm{m}} = 0$ and the radius function $v_k^{\mathrm{r}} = 3$. By using the traditional algorithm and the proposed algorithm, the filter error curves and filter error variance curves for the free-fall moving target tracking problem can be obtained, as shown in figures 6–8. Notice that the ideal error curve for target displacement is described by the reference line in figures 6 and 7. It can be found that, for both traditional and proposed algorithm, the displacement measurement error is considerably high and fails to converge, which is mainly attributed to the impact of the noise on the sensor's measurement. However, with the use of the filter algorithms, there is a notable reduction in the filter error of the displacement, and the filter errors of both displacement and velocity show a tendency to converge to zero.

In addition, the filter error variances for both the displacement and velocity converge to zero over time for both algorithms mentioned above, and the filter error variances calculated by these two algorithms have identical characteristics to reach convergence, primarily due to the fact that the parameters involving in the calculation of filter error covariance matrix such as Kalman gain measurement noise covariance matrix are the same. Table 1 lists the detail filter results of the

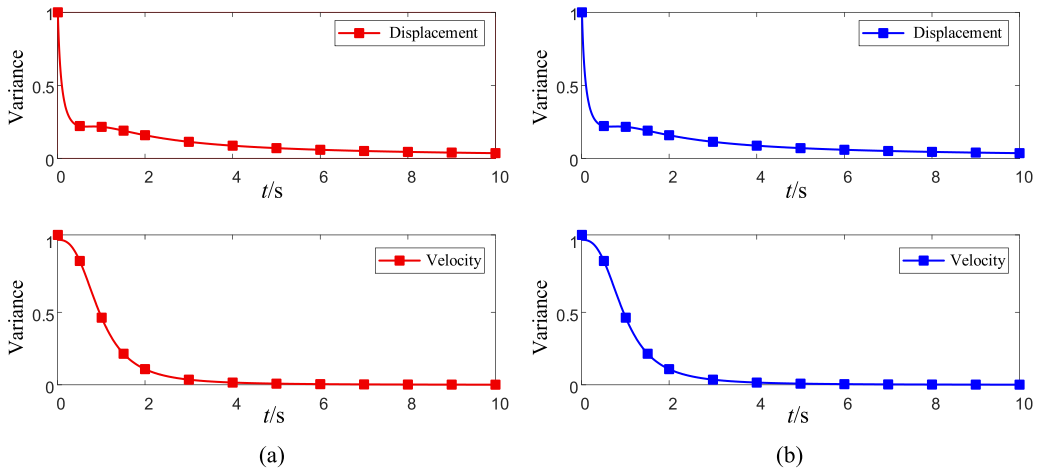


Figure 8. Filter error variance curves of state estimation for the free-fall moving target tracking problem using traditional and proposed algorithms. (a) Traditional algorithm; (b) proposed algorithm.

Table 1. The filter results of free-fall moving target tracking problem at different time points for traditional and proposed algorithms.

			Estimation value (relative error %)		Filter error variance	
System state	Time	True value	Traditional algorithm	Proposed algorithm	Traditional algorithm	Proposed algorithm
Displacement	5 s	−25.00	−24.45 (2.21)	−24.61 (1.56)	7.03×10^{-2}	7.03×10^{-2}
	6 s	−80.00	−79.38 (0.78)	−79.42 (0.73)	5.89×10^{-2}	5.89×10^{-2}
	7 s	−145.00	−144.27 (0.50)	−144.37 (0.44)	5.06×10^{-2}	5.06×10^{-2}
	8 s	−220.00	−219.17 (0.38)	−219.37 (0.29)	4.44×10^{-2}	4.44×10^{-2}
	9 s	−305.00	−304.09 (0.30)	−304.11 (0.29)	3.59×10^{-2}	3.59×10^{-2}
	10 s	−400.00	−398.99 (0.25)	−399.02 (0.25)	3.56×10^{-2}	3.56×10^{-2}
Velocity	5 s	−50.00	−49.88 (0.24)	−49.91 (0.18)	8.20×10^{-3}	8.20×10^{-3}
	6 s	−60.00	−59.89 (0.18)	−59.89 (0.19)	4.80×10^{-3}	4.80×10^{-3}
	7 s	−70.00	−69.89 (0.15)	−69.90 (0.14)	3.00×10^{-3}	3.00×10^{-3}
	8 s	−80.00	−79.89 (0.13)	−79.92 (0.10)	2.00×10^{-3}	2.00×10^{-3}
	9 s	−90.00	−89.90 (0.11)	−89.89 (0.12)	1.40×10^{-3}	1.40×10^{-3}
	10 s	−100.00	−99.90 (0.10)	−99.89 (0.11)	1.10×10^{-3}	1.10×10^{-3}

Table 2. The comparison of the results between the traditional Kalman filter algorithm and the proposed algorithm.

Method	Filter error	Filter error variance	Dependence on sufficient samples
Traditional algorithm	Low	Low	High
Proposed algorithm	Low	Low	Low

target at different time points, from which it can be found that both the relative error and filter error variance of the displacement and velocity decrease with time for both algorithms, and there exists a positive correlation between them to some extent. The filter results show that the proposed filter algorithm exhibits its robust convergence for the free-fall moving target tracking problem, and the filter error variance can be used to reflect the relative error of the estimation value compared to true value. The comparison of the results of the traditional Kalman filter algorithm and the proposed filter algorithm is listed in table 2.

Secondly, the influence of radius function of the measurement noise on the filter estimation is investigated. The noise is treated as an uncorrelated interval process $\{v_k \in v_k^{\mathrm{I}}, k = 1, 2, \cdots\}$ with the middle point function $v_k^{\mathrm{m}} = 0$ and the following three cases of radius function are considered: (a) $v_k^{\mathrm{r}} = 3$; (b) $v_k^{\mathrm{r}} = 6$; (c) $v_k^{\mathrm{r}} = 9$. By applying the proposed filter algorithm, the corresponding filter error variance for both the target's displacement and velocity in the three cases can be obtained, as shown in figure 9. From the results, it can be found that the filter error variances of the displacement decrease rapidly after a brief increase and ultimately reaches convergence, while the filter error variances of the velocity reach convergence directly without preceding fluctuations. In addition, the convergence rates of the filter error variances of both displacement and velocity decrease with the increase of the radius function of the noise. For example, the filter error variance of the velocity for the case of $v_k^{\mathrm{r}} = 3$ reaches convergence faster than that of $v_k^{\mathrm{r}} = 9$. Table 3 lists the filter error variances at $t = 10\,\mathrm{s}$ for the above three cases, and it can be found that the filter error variances for both the displacement

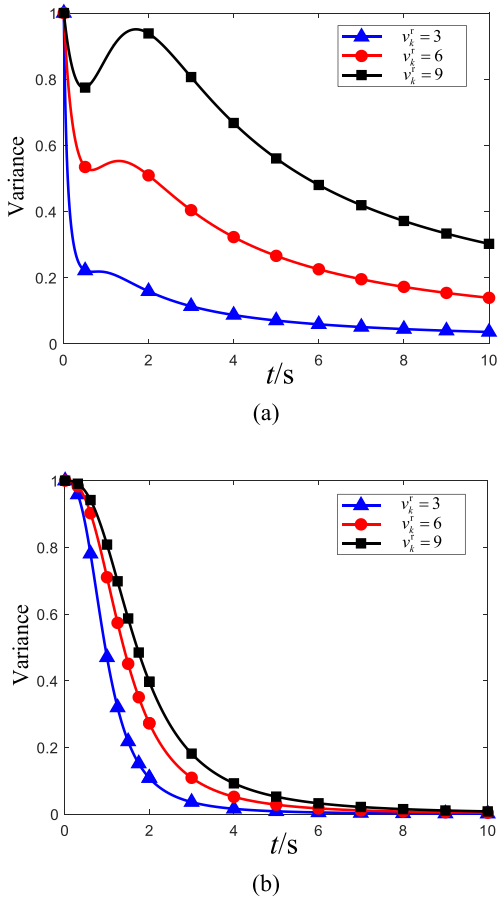


Figure 9. Filter error variance curves of state estimation for the free-fall moving target tracking problem under different radius functions. (a) Displacement; (b) velocity.

Table 3. Filter error variances of state estimation for the free-fall moving target tracking problem under different radius functions at $t = 10$s.

Radius function	Displacement	Velocity
Case a : $v_k^{\mathrm{r}} = 3$	3.56×10^{-2}	1.10×10^{-3}
Case b : $v_k^{\mathrm{r}} = 6$	1.39×10^{-1}	3.91×10^{-3}
Case c : $v_k^{\mathrm{r}} = 9$	3.02×10^{-1}	7.89×10^{-3}

and velocity increase with the increase of the radius function of the noise. The above results show that the radius function of the measurement noise has a significant impact on the filter estimation convergence rate.

4.2. A ship navigation and positioning problem

In the ship navigation and positioning problem, the GPS receiver captures real-time signals transmitted by the in-orbit navigation satellites, thereby determining the current position and velocity of the ship. To improve the accuracy of positioning, it is essential to filter the GPS measurement signals concerning the position and velocity of the ship. The state equation and measurement equation for the ship navigation and positioning problem can be simplified as [53].

$$\begin{cases} \mathbf{X}_k = \mathbf{\Phi}\mathbf{X}_{k-1} + \mathbf{\Gamma}\mathbf{W}_{k-1} \\ \mathbf{Z}_k = \mathbf{H}\mathbf{X}_k + \mathbf{V}_k \end{cases} \tag{54}$$

where $\mathbf{X}_k = [x_k,\ \dot{x}_k,\ y_k,\ \dot{y}_k]^{\mathrm{T}}$, x_k and $\dot{x}_k$ are the lateral position and velocity of the ship at the measurement time kT_0, respectively, y_k and $\dot{y}_k$ are the longitudinal position and velocity of the ship at the measurement time kT_0, respectively, T_0 is the measurement period; $\mathbf{W}_k = [\alpha_k,\ \beta_k]^{\mathrm{T}}$ is the process noise vector, where α_k and β_k are process noises related to the lateral and longitudinal maneuver, respectively; $\mathbf{V}_k = [\gamma_k,\ \eta_k]^{\mathrm{T}}$, where γ_k and η_k are the measurement noises for the GPS system in the lateral and longitudinal positions, respectively; $\mathbf{\Phi}$, $\mathbf{\Gamma}$ and $\mathbf{H}$ are given by:

$$\mathbf{\Phi} = \begin{bmatrix} 1 & T_0 & 0 & 0 \\ 0 & 1 & 0 & 0 \\ 0 & 0 & 1 & T_0 \\ 0 & 0 & 0 & 1 \end{bmatrix}, \mathbf{\Gamma} = \begin{bmatrix} 0.5T_0^2 & 0 \\ T & 0 \\ 0 & 0.5T_0^2 \\ 0 & T \end{bmatrix}, \mathbf{H} = \begin{bmatrix} 1 & 0 & 0 & 0 \\ 0 & 0 & 1 & 0 \end{bmatrix}. \tag{55}$$

The measurement period of GPS receiver is $T_0 = 1$s and the total measurement time is 200s. The initial system state is set as an interval vector with the middle point vector $\mathbf{X}_0^{\mathrm{m}} = [0,\ 2,\ 0,\ -10]^{\mathrm{T}}$ and the covariance matrix:

$$\mathbf{P}_0 = \begin{bmatrix} 1 & 0 & 0 & 0 \\ 0 & 1 & 0 & 0 \\ 0 & 0 & 1 & 0 \\ 0 & 0 & 0 & 1 \end{bmatrix}. \tag{56}$$

The measurement noise vector is treated as an uncorrelated interval process vector $\mathbf{V}_k^{\mathrm{I}}$ with the middle point function vector $\mathbf{V}_k^{\mathrm{m}} = [0,\ 0]^{\mathrm{T}}$ and the radius function vector $\mathbf{V}_k^{\mathrm{r}} = [0.01,\ 0.01]^{\mathrm{T}}$.

Firstly, the convergence of the proposed filter algorithm in the state estimation for the ship navigation and positioning problem is investigated. The process noise is considered as an uncorrelated interval process vector $\mathbf{W}_k^{\mathrm{I}}$ with the middle point function vector $\mathbf{W}_k^{\mathrm{m}} = [0,\ 0]^{\mathrm{T}}$ and the radius function vector $\mathbf{W}_k^{\mathrm{r}} = [0.01,\ 0.01]^{\mathrm{T}}$. By using the proposed filter algorithm, the filter results can be obtained, as shown in figures 10–12. It can be found that the ship navigates in uniform rectilinear trajectory, and its estimation trajectory closely approximates the true trajectory, as shown in figure 11. In addition, for both the lateral position and lateral velocity of the ship, the filter error variances consistently remain below the prediction error variances. The filter error variances of both lateral position and lateral velocity ultimately achieve convergence, with the final convergence value almost the same as the prediction error variance, as shown in figure 10. This occurs mainly because the radius functions of the process noises are small, resulting in relatively small prediction error variances estimated directly through the system state equation. Moreover, the root mean

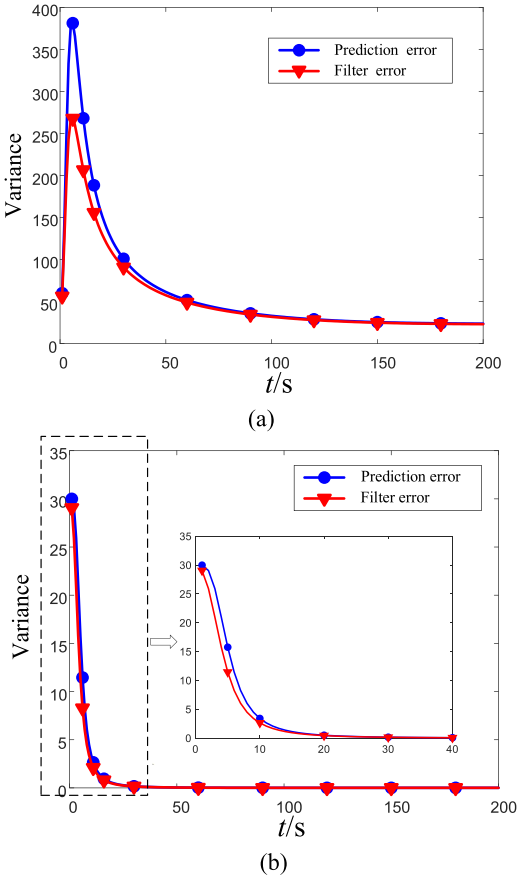


Figure 10. Prediction and filter error variance curves of state estimation for the ship. (a) Lateral position; (b) Lateral velocity.

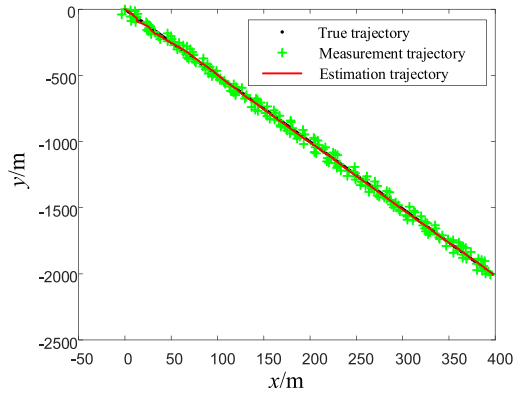


Figure 11. Plane tracking trajectory of the ship.

square errors (RMSEs) of lateral position and lateral velocity for the ship show a decreasing trend over time and eventually reach convergence, as shown in figure 12, indicating that the proposed filter algorithm possesses high tracking accuracy and exhibits good convergence. While the noise cannot be entirely filtered out, the proposed algorithm can effectively reduce the impact of noise on the state estimation for the ship.

Secondly, the influence of radius functions for process noises on the ship state estimation is investigated. Let the process noises as an uncorrelated interval process vector $\mathbf{W}_k^{\mathrm{I}}$ with the middle point function vector $\mathbf{W}_k^{\mathrm{m}} = [0,\ 0]^{\mathrm{T}}$. Consider

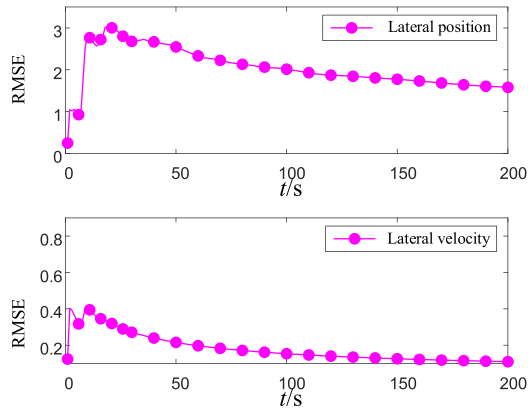


Figure 12. Root mean square error curves of state estimation for the ship.

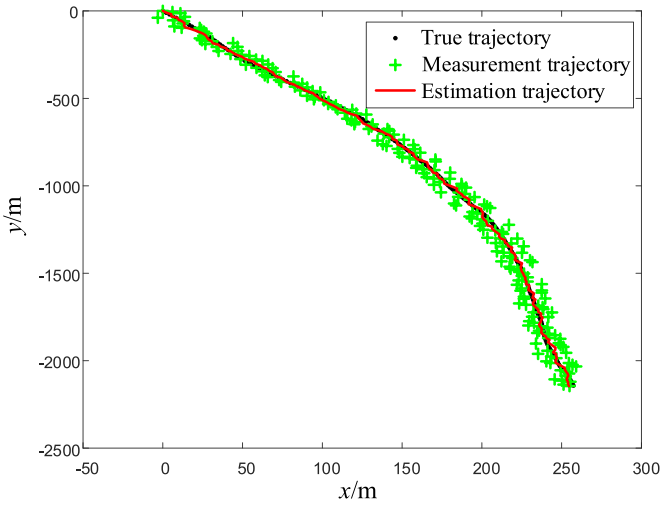


Figure 13. Plane tracking trajectory of the ship when $\mathbf{W}_k^{\mathrm{r}} = [0.5,\ 0.5]^{\mathrm{T}}$.

the following two cases of radius function vectors: (a) $\mathbf{W}_k^{\mathrm{r}} = [0.5,\ 0.5]^{\mathrm{T}}$; (b) $\mathbf{W}_k^{\mathrm{r}} = [2,\ 2]^{\mathrm{T}}$. By using the proposed filter algorithm, the corresponding filter results of the ship for the above two cases can be obtained, as shown in figures 13–16. It can be found that when the radius functions of the process noises increase, the ship no longer moves in a straight line at uniform velocity approximately, but shows variations in the motion trajectory, as shown in figures 13 and 15. For the above two cases, the estimation trajectories of the ship are close to the true ones, showing that the proposed filter algorithm is effective for tracking not only the target moving at a uniform or approximately uniform velocity but also that with greater mobility. In addition, as shown in figures 14 and 16, the filter error variances for the lateral position and lateral velocity achieve convergence for both of the above cases. Nevertheless, it can be found that the increase of the radius functions of the process noises causes a rise of the convergence value for both the prediction error variance and filter error variance of the ship state. For instance, the filter error variance in convergence stage of the lateral position for the ship when $\mathbf{W}_k^{\mathrm{r}} = [2,\ 2]^{\mathrm{T}}$ are obviously greater than that when

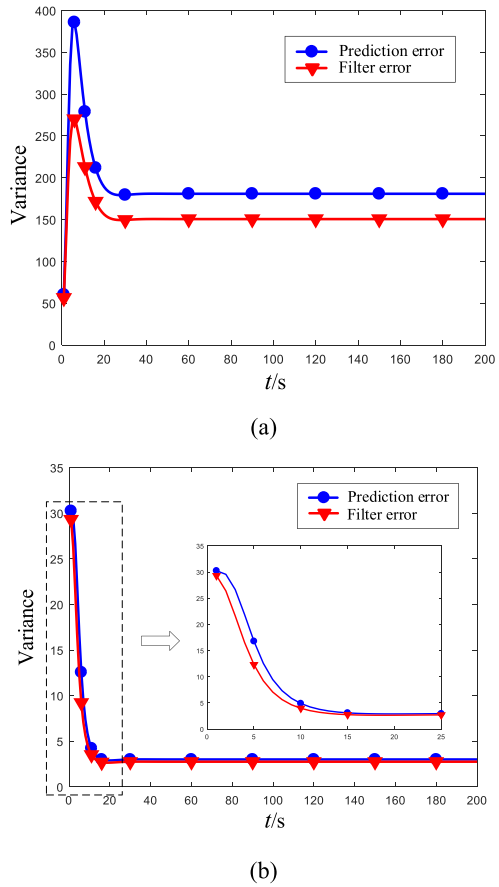


Figure 14. Prediction and filter error variance curves of state estimation for the ship when $\mathbf{W}_k^{\mathrm{r}} = [0.5,\ 0.5]^{\mathrm{T}}$. (a) Lateral position; (b) Lateral velocity.

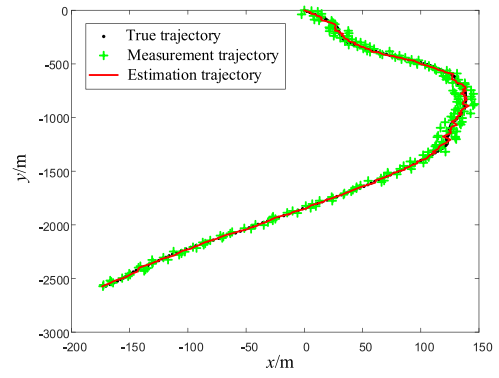


Figure 15. Plane tracking trajectory of the ship when $\mathbf{W}_k^{\mathrm{r}} = [2,\ 2]^{\mathrm{T}}$.

$\mathbf{W}_k^{\mathrm{r}} = [0.5,\ 0.5]^{\mathrm{T}}$, as observed by comparing figure 14(a) with figure 16(a). In summary, the above phenomena indicate that the radius function of process noises has significant impact on the prediction error variances and the filter error variances of the system state.

4.3. A strapdown inertial navigation system (SINS) problem

The inertial navigation system (INS) employs sensors such as accelerometers and gyroscopes to measure the acceleration

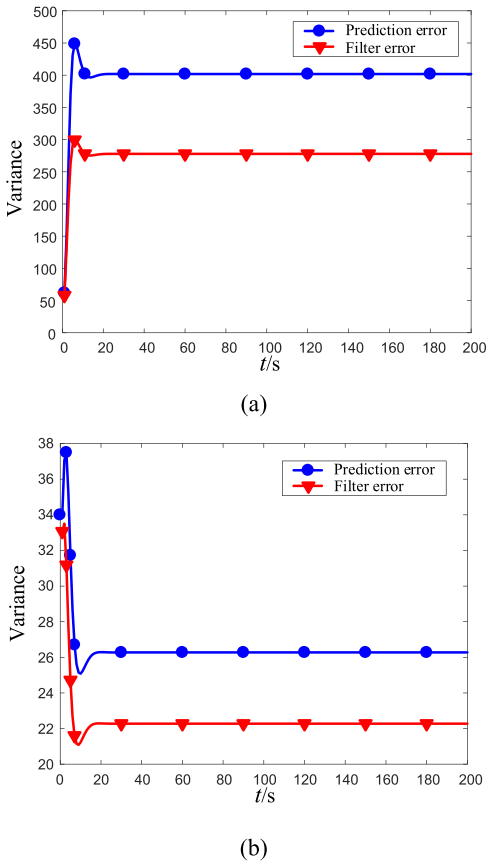


Figure 16. Prediction and filter error variance curves of state estimation for the ship when $\mathbf{W}_k^{\mathrm{r}} = [2,\ 2]^{\mathrm{T}}$. (a) Lateral position; (b) lateral velocity.

and attitude angles of the carrier, thereby providing positional information. Owing to strong resistance to external disturbances, INS has been widely applied in aerospace, aviation, and various civilian domains, as well as in national defense technologies [54]. With the advancement of sophisticated computer technologies, an improved form of the INS, namely the SINS, has been proposed. The SINS eliminates the traditional electromechanical platform and instead computes the attitude information of the vehicle through a mathematical platform established within the computer, thereby simplifying the overall system architecture. The SINS, owing to its high reliability and low maintenance cost, has gradually become the mainstream configuration. The initial alignment process of SINS constitutes a critical stage in the overall navigation procedure, as the effective control of alignment errors directly determines the accuracy and stability of the system.

Under static conditions, the state and measurement equations of the initial alignment error for the system are established [55]:

$$\begin{cases} \dot{\mathbf{X}}(t) = \mathbf{A}(t)\mathbf{X}(t) + \mathbf{W}(t) = \begin{bmatrix} \mathbf{F} & \mathbf{C} \\ \mathbf{0}_{5\times5} & \mathbf{0}_{5\times5} \end{bmatrix} \mathbf{X}(t) + \mathbf{W}(t) \\ \mathbf{Z}(t) = \mathbf{H}(t)\mathbf{X}(t) + \mathbf{V}(t) \end{cases} \tag{57}$$

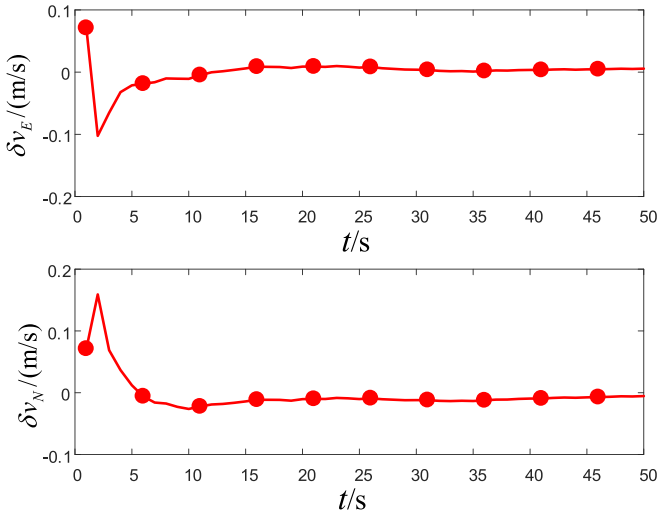


Figure 17. The initial alignment velocity error curves under static base conditions.

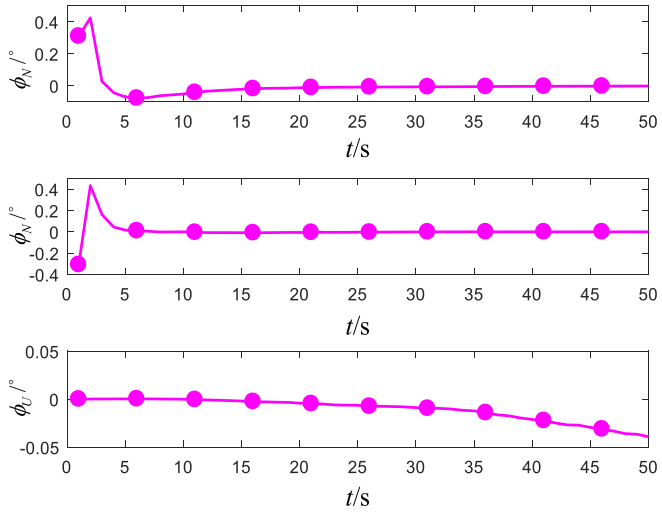


Figure 18. The initial alignment misalignment angle curves under static base conditions.

where $\mathbf{X}(t) = [\delta v_{\mathrm{E}}, \delta v_{\mathrm{N}}, \phi_{\mathrm{E}}, \phi_{\mathrm{N}}, \phi_{\mathrm{U}}, \varepsilon_{\mathrm{E}}, \varepsilon_{\mathrm{N}}, \varepsilon_{\mathrm{U}}, \nabla_{\mathrm{E}}, \nabla_{\mathrm{N}}]^{\mathrm{T}}$ denotes state vector, δv_{E} and δv_{N} denote the velocity error components in the eastward and northward directions, respectively, ϕ_{E}, ϕ_{N} and ϕ_{U} represent the misalignment angles in the east, north, and upward directions, respectively, ε_{E}, ε_{N}, and ε_{U} correspond to the accelerometer biases in the east, north, and upward directions, respectively, ∇_{E} and ∇_{N} denote the constant gyro drifts in the eastward and northward directions, respectively; $\mathbf{C} = \mathbf{I}_{5\times5}$ denotes the attitude matrix, $\mathbf{I}_{p\times p}$ denotes the $p \times p$ identity matrix; $\mathbf{W}(t) = [\eta_{\delta v_{\mathrm{E}}}, \eta_{\delta v_{\mathrm{N}}}, \eta_{\phi_{\mathrm{E}}}, \eta_{\phi_{\mathrm{N}}}, \eta_{\phi_{\mathrm{U}}}, 0, 0, 0, 0, 0]^{\mathrm{T}}$ denotes the state noise vector; $\mathbf{Z}(t) = [v_{\mathrm{E}}, v_{\mathrm{N}}]^{\mathrm{T}}$ denotes the measurement vector; $\mathbf{H}(t) = [\mathbf{I}_{2\times2}, \mathbf{0}_{2\times8}]$ denotes the coefficient matrix; $\mathbf{V}(t) = [\mu_{\mathrm{E}}, \mu_{\mathrm{N}}]^{\mathrm{T}}$ denotes the measurement noise vector; $\mathbf{F}$ is:

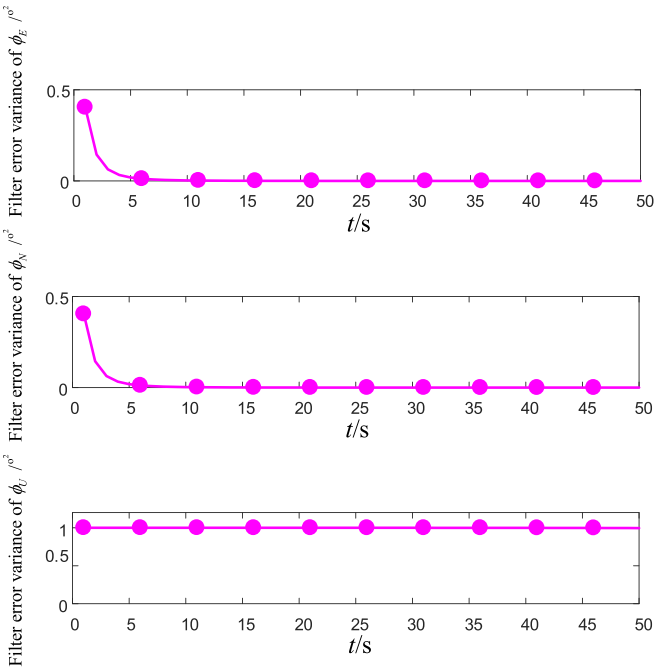


Figure 19. Filter error variance curves of the initial alignment misalignment angle under static base conditions.

$$\mathbf{F} = \begin{bmatrix} 0 & 2\Omega\sin\varphi & 0 & -g & 0 \\ -2\Omega\sin\varphi & 0 & g & 0 & 0 \\ 0 & 0 & 0 & \Omega\sin\varphi & -\Omega\cos\varphi \\ 0 & 0 & -\Omega\sin\varphi & 0 & 0 \\ 0 & 0 & \Omega\cos\varphi & 0 & 0 \end{bmatrix} \tag{58}$$

where φ, Ω and g denote the local latitude, the Earth's rotation rate and the gravitational acceleration, respectively.

By discretizing the state and measurement equations of the aforementioned initial alignment error system, the following discrete equation are obtained [55]:

$$\begin{aligned} \mathbf{P}_0 = \mathrm{diag}\Big\{ &(0.1\,\mathrm{m\,s^{-1}})^2,\ (0.1\,\mathrm{m\,s^{-1}})^2,\ (1^\circ)^2,\ (1^\circ)^2,\ (1^\circ)^2, \\ &\times\ (0.02^\circ\mathrm{h^{-1}})^2,\ (0.02^\circ\mathrm{h^{-1}})^2,\ (0.02^\circ\mathrm{h^{-1}})^2,\ (100\mu g)^2, (100\mu g)^2 \Big\} \end{aligned} \tag{59}$$

where $\mathrm{diag}\{\cdot\}$ denotes the diagonal matrix operator. Consider the process noise and measurement noise as uncorrelated interval processes $\mathbf{W}_k^{\mathrm{I}}$ and $\mathbf{V}_k^{\mathrm{I}}$, respectively, with midpoint function vectors $\mathbf{W}_k^{\mathrm{m}} = [0, 0, 0, 0, 0, 0, 0, 0, 0, 0]^{\mathrm{T}}$ and $\mathbf{V}_k^{\mathrm{m}} = [0, 0]^{\mathrm{T}}$, and radius function vectors $\mathbf{W}_k^{\mathrm{r}} = \left[50\mu g, 50\mu g, 50\mu g, 0.1^\circ\mathrm{h^{-1}}, 0.1^\circ\mathrm{h^{-1}}, 0, 0, 0, 0, 0\right]^{\mathrm{T}}$ and $\mathbf{V}_k^{\mathrm{r}} = \left[0.1\,\mathrm{m\,s^{-1}}, 0.1\,\mathrm{m\,s^{-1}}\right]^{\mathrm{T}}$. Let the filter period be $T_0 = 1\,\mathrm{s}$ and the location be at latitude $\varphi = 45^\circ$ North. The initial misalignment angles are assumed to be $\phi_{\mathrm{E}} = 1^\circ$, $\phi_{\mathrm{N}} = 1^\circ$ and $\phi_{\mathrm{U}} = 1^\circ$.

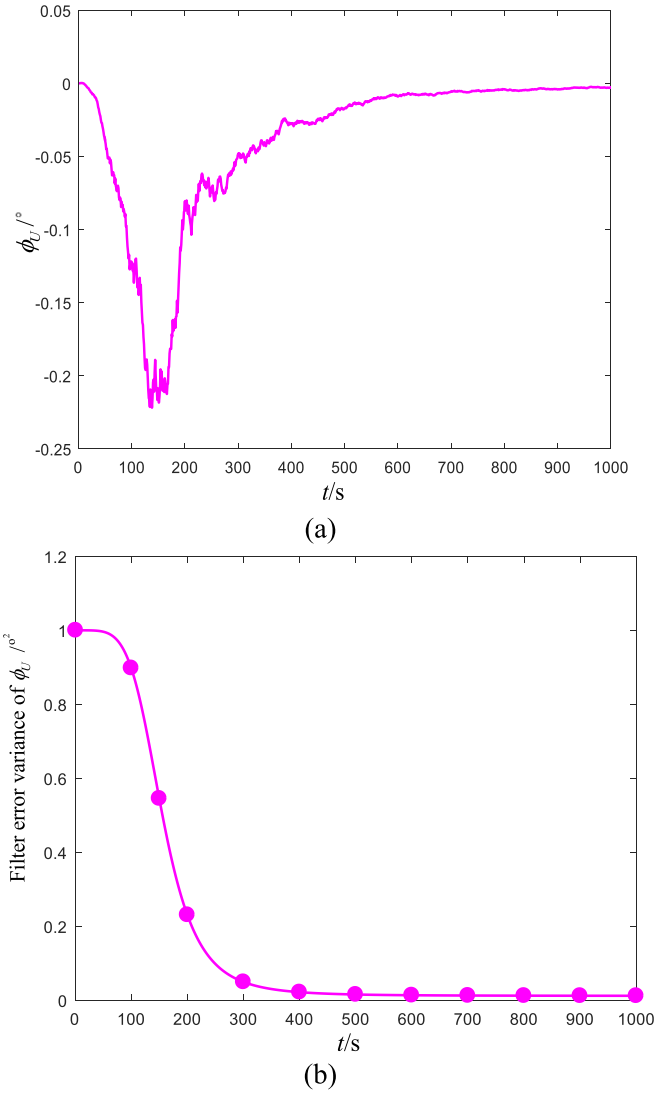


Figure 20. Filter results of the initial alignment upward misalignment angle under static base conditions. (a) The upward misalignment angle; (b) filter error variance curve of the upward misalignment angle.

The convergence characteristics of the proposed filter algorithm in state estimation of the system are investigated. By utilizing the proposed algorithm, the filter results of the SINS within 50 s are obtained, the curves of the results are illustrated in figures 17–19. It can be observed from the results that, under the initial conditions of the static base, the filter estimations of the eastward and northward velocity errors tend towards zero. The filter estimations of the eastward and northward misalignment angles reach the convergence stage. While the filter estimation of the upward misalignment angle consistently decreases throughout the entire filtering process without reaching the convergence stage. Therefore, the total filter duration is set to 1000 s, and the filter results of the upward misalignment angle are obtained, as shown in figure 20. From the results it can be known that the upward misalignment angle eventually reaches the convergence stage. This phenomenon indicates that the filter estimation of the eastward and northward misalignment angles performs well, with faster alignment speeds, while the alignment speed of the upward misalignment angle is significantly slower compared to the first two. This is primarily because the convergence speed of the filter is related to the noise level. Only accelerometer biases cause estimation errors for the eastward and northward misalignment angles, whereas the estimation errors of the upward misalignment angle are affected by both the biases of the northward misalignment angle and the constant drift of the eastward gyroscope, resulting in larger errors. Therefore, the observability of the upward misalignment angle is not as good as that of the eastward and northward misalignment angles. The filter results above demonstrate that the proposed filter algorithm can effectively control the initial alignment errors of the SINS, thereby ensuring the accuracy of the navigation system's subsequent positioning.

5. Conclusions

This paper proposes a new Kalman filter algorithm based on the interval process model for linear discrete systems. By utilizing the interval process model to describe the uncertainty of the noise, the dependence of the analysis on extensive samples can be greatly reduced. Through the numerical examples, the following phenomena can be found. First, the filter errors, prediction error variances, filter error variances, and RMSEs of the system state all show a decreasing trend over time and eventually converge. Second, the radius function of the process noise affects the filter estimation, with the filter error variance convergence value increasing as the radius function of the noise increases. Third, although the noise cannot be completely filtered out, the adverse effects of noise on state estimation can be effectively mitigated through the proposed algorithm. Currently, noise is assumed to be an uncorrelated interval process in linear dynamic system problems. We will further explore the filter analysis with correlated interval process noises in practical engineering scenarios such as multisensor systems, striving to overcome the difficulties of estimation performance degradation, promising more advancements in the field of parameter estimation.

Acknowledgment

This work is supported by the National Key Research and Development Program of China (Grant No. 2024YFF0505101), the State Key Program of National Science Foundation of China (52235005), and the XPLORER PRIZE from Tencent, the National Natural Science Foundation of China (Grant No. 52575270).

Conflict of interest

The authors declare that they have no conflict of interest.

Appendix

According to equation (1), the state prediction estimation of $\mathbf{X}_k$ can be obtained:

$$\hat{\mathbf{X}}_{k,k-1} = \mathbf{\Phi}_{k,k-1}\hat{\mathbf{X}}_{k-1} + \mathbf{\Psi}_{k,k-1}\mathbf{U}_{k-1} \tag{A.1}$$

and the prediction estimation of $\mathbf{Z}_k$ can be obtained:

$$\hat{\mathbf{Z}}_{k,k-1} = \mathbf{H}_k\hat{\mathbf{X}}_{k,k-1}. \tag{A.2}$$

The measurement residual vector between $\mathbf{Z}_k$ and $\hat{\mathbf{Z}}_{k,k-1}$ is defined as:

$$\tilde{\mathbf{Z}}_{k,k-1} = \mathbf{Z}_k - \hat{\mathbf{Z}}_{k,k-1} = \mathbf{Z}_k - \mathbf{H}_k\hat{\mathbf{X}}_{k,k-1}. \tag{A.3}$$

By using the measurement residual vector $\tilde{\mathbf{Z}}_{k,k-1}$ to correct the original state prediction estimation $\hat{\mathbf{X}}_{k,k-1}$, the optimal filter estimation at the time step k can be obtained:

$$\hat{\mathbf{X}}_k = \hat{\mathbf{X}}_{k,k-1} + \mathbf{K}_k\left(\mathbf{Z}_k - \mathbf{H}_k\hat{\mathbf{X}}_{k,k-1}\right) \tag{A.4}$$

where $\mathbf{K}_k$ is the filter gain matrix.

The prediction error $\mathbf{e}_{k,k-1}$ and the filter error $\mathbf{e}_k$ are, respectively, defined as:

$$\mathbf{e}_{k,k-1} = \mathbf{X}_k - \hat{\mathbf{X}}_{k,k-1} \tag{A.5}$$

$$\mathbf{e}_k = \mathbf{X}_k - \hat{\mathbf{X}}_k. \tag{A.6}$$

Substitute equations (1) and (A.1) into equation (A.5) yields:

$$\mathbf{e}_{k,k-1} = \mathbf{\Phi}_{k,k-1}\left(\mathbf{X}_{k-1} - \hat{\mathbf{X}}_{k-1}\right) + \mathbf{\Gamma}_{k,k-1}\mathbf{W}_{k-1}. \tag{A.7}$$

Substitute equations (1) and (A.4) into equation (A.6) yields:

$$\mathbf{e}_k = \left[\mathbf{I} - \mathbf{K}_k\mathbf{H}_k\right]\left(\mathbf{X}_k - \hat{\mathbf{X}}_{k,k-1}\right) + \mathbf{K}_k\mathbf{V}_k. \tag{A.8}$$

According to equation (A.7), the covariance matrix of the prediction error $\mathbf{e}_{k,k-1}$ can be obtained:

$$\begin{aligned}\mathbf{P}_{k,k-1} &= \mathbf{Cov}\left(\mathbf{e}_{k,k-1}, \mathbf{e}_{k,k-1}\right)\\ &= \mathbf{\Phi}_{k,k-1}\mathbf{Cov}\left(\mathbf{X}_{k-1} - \hat{\mathbf{X}}_{k-1}, \mathbf{X}_{k-1} - \hat{\mathbf{X}}_{k-1}\right)\mathbf{\Phi}_{k,k-1}^{\mathrm{T}}\\ &\quad + \mathbf{\Phi}_{k,k-1}\mathbf{Cov}\left(\mathbf{X}_{k-1} - \hat{\mathbf{X}}_{k-1}, \mathbf{W}_{k-1}\right)\mathbf{\Gamma}_{k,k-1}^{\mathrm{T}}\\ &\quad + \mathbf{\Gamma}_{k,k-1}\mathbf{Cov}\left(\mathbf{W}_{k-1}, \mathbf{X}_{k-1} - \hat{\mathbf{X}}_{k-1}\right)\mathbf{\Phi}_{k,k-1}^{\mathrm{T}}\\ &\quad + \mathbf{\Gamma}_{k,k-1}\mathbf{Cov}\left(\mathbf{W}_{k-1}, \mathbf{W}_{k-1}\right)\mathbf{\Gamma}_{k,k-1}^{\mathrm{T}}.\end{aligned} \tag{A.9}$$

It can be proved that $\mathbf{Cov}\left(\mathbf{X}_{k-1} - \hat{\mathbf{X}}_{k-1}, \mathbf{W}_{k-1}\right) = \mathbf{0}_{n_1\times n_1}$, and equation (A.9) can be simplified as

$$\mathbf{P}_{k,k-1} = \mathbf{\Phi}_{k,k-1}\mathbf{P}_{k-1}\mathbf{\Phi}_{k,k-1}^{\mathrm{T}} + \mathbf{\Gamma}_{k,k-1}\mathbf{Q}_{k-1}\mathbf{\Gamma}_{k,k-1}^{\mathrm{T}}. \tag{A.10}$$

According to equation (A.8), the covariance matrix of the filter error $\mathbf{e}_k$ can be obtained:

$$\begin{aligned}\mathbf{P}_k &= \mathbf{Cov}\left(\mathbf{e}_k, \mathbf{e}_k\right)\\ &= \left(\mathbf{I} - \mathbf{K}_k\mathbf{H}_k\right)\mathbf{Cov}\left(\mathbf{X}_k - \hat{\mathbf{X}}_{k,k-1}, \mathbf{X}_k - \hat{\mathbf{X}}_{k,k-1}\right)\left(\mathbf{I} - \mathbf{K}_k\mathbf{H}_k\right)^{\mathrm{T}}\\ &\quad - \left(\mathbf{I} - \mathbf{K}_k\mathbf{H}_k\right)\mathbf{Cov}\left(\mathbf{X}_k - \hat{\mathbf{X}}_{k,k-1}, \mathbf{V}_k\right)\mathbf{K}_k^{\mathrm{T}}\\ &\quad - \mathbf{K}_k\mathbf{Cov}\left(\mathbf{V}_k, \mathbf{X}_k - \hat{\mathbf{X}}_{k,k-1}\right)\left(\mathbf{I} - \mathbf{K}_k\mathbf{H}_k\right)^{\mathrm{T}}\\ &\quad + \mathbf{K}_k\mathbf{Cov}\left(\mathbf{V}_k, \mathbf{V}_k\right)\mathbf{K}_k^{\mathrm{T}}.\end{aligned} \tag{A.11}$$

It can be proved that $\mathbf{Cov}\left(\mathbf{X}_k - \hat{\mathbf{X}}_{k,k-1}, \mathbf{V}_k\right) = \mathbf{0}_{n_1\times n_2}$, and equation (A.11) can be simplified as:

$$\mathbf{P}_k = \left(\mathbf{I} - \mathbf{K}_k\mathbf{H}_k\right)\mathbf{P}_{k,k-1}\left(\mathbf{I} - \mathbf{K}_k\mathbf{H}_k\right)^{\mathrm{T}} + \mathbf{K}_k\mathbf{R}_k\mathbf{K}_k^{\mathrm{T}}. \tag{A.12}$$

The gain matrix $\mathbf{K}_k$ for a minimum filter error variance should minimize the sum of diagonal elements of $\mathbf{P}_k$, namely the trace of $\mathbf{P}_k$:

$$\begin{aligned}\mathrm{tr}\left(\mathbf{P}_k\right) &= \mathrm{tr}\left(\mathbf{P}_{k,k-1}\right) - 2\mathrm{tr}\left(\mathbf{K}_k\mathbf{H}_k\mathbf{P}_{k,k-1}\right)\\ &\quad + \mathrm{tr}\left(\mathbf{K}_k\left(\mathbf{H}_k\mathbf{P}_{k,k-1}\mathbf{H}_k^{\mathrm{T}} + \mathbf{R}_k\right)\mathbf{K}_k^{\mathrm{T}}\right).\end{aligned} \tag{A.13}$$

Take the derivative of $\mathrm{tr}\left(\mathbf{P}_k\right)$ with respect to $\mathbf{K}_k$ yields:

$$\begin{aligned}\frac{\partial\mathrm{tr}\left(\mathbf{P}_k\right)}{\partial\mathbf{K}_k} &= \frac{\partial\mathrm{tr}\left(-2\mathbf{K}_k\mathbf{H}_k\mathbf{P}_{k,k-1}\right)}{\partial\mathbf{K}_k} + \frac{\partial\mathrm{tr}\left(\mathbf{K}_k\left(\mathbf{H}_k\mathbf{P}_{k,k-1}\mathbf{H}_k^{\mathrm{T}} + \mathbf{R}_k\right)\mathbf{K}_k^{\mathrm{T}}\right)}{\partial\mathbf{K}_k}\\ &= -2\left(\mathbf{H}_k\mathbf{P}_{k,k-1}\right)^{\mathrm{T}} + 2\mathbf{K}_k\left(\mathbf{H}_k\mathbf{P}_{k,k-1}\mathbf{H}_k^{\mathrm{T}} + \mathbf{R}_k\right).\end{aligned} \tag{A.14}$$

Let equation (A.14) be equal to $\mathbf{0}_{n_1\times n_2}$, then $\mathbf{K}_k$ can be solved as:

$$\mathbf{K}_k = \mathbf{P}_{k,k-1}\mathbf{H}_k^{\mathrm{T}}\left(\mathbf{H}_k\mathbf{P}_{k,k-1}\mathbf{H}_k^{\mathrm{T}} + \mathbf{R}_k\right)^{-1}. \tag{A.15}$$

References

[1] Wiener N 1949 *Extrapolation, Interpolation, and Smoothing of Stationary Time Series: With Engineering Applications* (MIT Press)

[2] Kalman R E 1960 A new approach to linear filtering and prediction problems *J. Basic Eng.* **82** 35–45

[3] Kalman R E and Bucy R S 1961 New results in linear filtering and prediction theory *J. Basic Eng.* **83** 95–108

[4] Zakai M 1959 On a property of Wiener filters *IRE Trans. Inf. Theory* **5** 15–17

[5] Khodarahmi M and Maihami V 2023 A review on Kalman filter models *Arch. Comput. Methods Eng.* **30** 727–47

[6] Li X, Liang J, Huang G, Ma S and Li H 2024 Adaptive invariant extended Kalman filter-based tightly-coupled SINS/RTK-integrated positioning for rotor unmanned aerial vehicle *IEEE Trans. Instrum. Meas.* **73** 1–17

[7] Jafari H and Poshtan J 2021 Event-triggered robust fault diagnosis Kalman filter for stochastic systems *IEEE Sens. J.* **21** 11031–9

[8] Su Y, Han J, Ma C, Wu J, Wang X, Zhu Q and Shen J 2024 Adaptive Kalman filter based on online ARW estimation for compensating low-frequency error of MHD ARS *IEEE Trans. Instrum. Meas.* **73** 1–10

[9] Diaz M, Charbonnel P É and Chamoin L 2023 A new Kalman filter approach for structural parameter tracking: application to the monitoring of damaging structures tested on shaking-tables *Mech. Syst. Signal Process* **182** 109529

[10] Fahmy H M, Hasanien H M, Alharbi M and Ji H 2025 Hybrid extended Kalman filter with Newton Raphson method for lifetime prediction of lithium-ion batteries *Sci. Rep.* **15** 14592

[11] Afrasiabi A, Faramarzi A, Chapman D and Keshavarzi A 2025 Optimising ground penetrating radar data interpretation: a hybrid approach with AI-assisted Kalman filter and wavelet transform for detecting and locating buried utilities *J. Appl. Geophys.* **232** 105567

[12] Guo M, Hao Y, Lu Y and Sun L 2025 Long-short term memory modeling and performance analysis of extended-state Kalman filter-based energy-saving model predictive control for supercritical unit *Appl. Therm. Eng.* **272** 126202

[13] Gao G, Yi Y, Zhong Y, Liang S, Hu G and Gao B 2025 A robust Kalman filter based on kernel density estimation for system state estimation against measurement outliers *IEEE Trans. Instrum. Meas.* **74** 1–12

[14] Elliott A J, Nakhaeezadeh Gutierrez A, Felicetti L and Zanotti Fragonara L 2025 In-orbit system identification of a flexible satellite with variable mass using dual unscented Kalman filters *Acta Astronaut.* **226** 71–86

[15] Gu H, Li Y, Jiang L and Luo Z 2025 A generalized approach for remaining useful life prediction considering the multi-source uncertainty of mechanical systems *J. Reliab. Sci. Eng.* **1** 025301

[16] Huang Y, Zhang Y, Xu B, Wu Z and Chambers J A 2018 A new adaptive extended Kalman filter for cooperative localization *IEEE Trans. Aerosp. Electron. Syst.* **54** 353–68

[17] Davari N and Gholami A 2019 Variational Bayesian adaptive Kalman filter for asynchronous multirate multi-sensor integrated navigation system *Ocean Eng.* **174** 108–16

[18] Shan C, Zhou W, Yang Y and Jiang Z 2021 Multi-fading factor and updated monitoring strategy adaptive Kalman filter-based variational Bayesian *Sensors* **21** 198

[19] Fu H and Cheng Y 2022 A novel maximum likelihood and moving weighted average based adaptive Kalman filter *J. Instrum.* **17** 08036

[20] Assa A and Plataniotis K N 2017 Adaptive Kalman filtering by covariance sampling *IEEE Signal Process Lett.* **24** 1288–92

[21] Wang H, Deng Z, Feng B, Ma H and Xia Y 2017 An adaptive Kalman filter estimating process noise covariance *Neurocomputing* **223** 12–17

[22] Hu J and Shi X 2021 Refined alignment method for single-axis rotary inertial navigation based on fuzzy adaptive filtering *J. Sys. Simul.* **33** 315–23

[23] Pan Z, Yi X, Zhang Y, Jeon B and Kwong S 2020 Efficient in-loop filtering based on enhanced deep convolutional neural networks for HEVC *IEEE Trans. Image Process* **29** 5352–66

[24] Assa A, Janabi-Sharifi F and Plataniotis K N 2019 Sample-based adaptive Kalman filtering for accurate camera pose tracking *Neurocomputing* **333** 307–18

[25] Liu Y, Fan X, Lv C, Wu J, Li L and Ding D 2018 An innovative information fusion method with adaptive Kalman filter for integrated INS/GPS navigation of autonomous vehicles *Mech. Syst. Signal Process.* **100** 605–16

[26] Zhou W, Li X, Yi J and He H 2019 A novel UKF-RBF method based on adaptive noise factor for fault diagnosis in pumping unit *IEEE Trans. Ind. Inf.* **15** 1415–24

[27] Ge Q, Li H and Wen C 2019 Deep analysis of Kalman filtering theory for engineering applications *J. Command Control* **5** 167–80

[28] Ge Q, Li Y, Wang Y, Hu X, Li H and Sun C 2024 Adaptive Kalman filtering based on model parameter ratios *IEEE Trans. Autom. Control* **69** 6230–7

[29] Etter D, Hicks M and Cho K 1982 Recursive adaptive filter design using an adaptive genetic algorithm *ICASSP'82. IEEE Int. Conf. on Acoustics, Speech, and Signal Processing* pp 635–8

[30] Sarkka S and Nummenmaa A 2009 Recursive noise adaptive Kalman filtering by variational Bayesian approximations *IEEE Trans. Autom. Control* **54** 596–600

[31] Zhang D, Zhang H, Zhou P, Li X-A, Wang F and Han X 2025 Time-variant system reliability analysis via stochastic process discretization and most probable point trajectory approximation *J. Reliab. Sci. Eng.* **1** 025001

[32] Ge Q, Shao T, Chen S and Wen C 2017 Carrier tracking estimation analysis by using the extended strong tracking filtering *IEEE Trans. Ind. Electron* **64** 1415–24

[33] Ge Q, Shao T, Duan Z and Wen C 2016 Performance analysis of the Kalman filter with mismatched noise covariances *IEEE Trans. Autom. Control* **61** 4014–9

[34] Chen G, Wang J and Shieh L S 1997 Interval Kalman filtering *IEEE Trans. Aerosp. Electron. Syst.* **33** 250–9

[35] Jun X, Carine J, Louise T-M and Françoise L G 2013 Fault detection using interval Kalman filtering enhanced by constraint propagation *52nd IEEE Conf. on Decision and Control* pp 490–5

[36] Andrew A M 2002 Applied interval analysis: with examples in parameter and state estimation, robust control and robotics *Kybernetes* **31** 1

[37] Tran T A, Jauberthie C, Gall F L and Travé-Massuyès L 2017 Interval Kalman filter enhanced by positive definite upper bounds *IFAC-PapersOnLine* **50** 1595–600

[38] Lu Q-H, Fergani S, Jauberthie C and Le Gall F 2019 Optimally bounded interval Kalman filter *2019 IEEE 58th Conf. on Decision and Control (CDC)* pp 379–84

[39] Lu Q-H, Fergani S and Jauberthie C 2021 A new scheme for fault detection based on optimal upper bounded interval Kalman filter *IFAC-PapersOnLine* **54** 292–7

[40] Lu Q-H, Fergani S and Jauberthie C 2024 Analytical bounds for an interval Kalman filter *IEEE Trans. Autom. Control* **69** 449–54

[41] Li X, Wang X, Qian J and Jiang G-P 2024 Improving interval Kalman filtering through interval optimization strategy *Proc. 2023 7th Chinese Conf. on Swarm Intelligence and Cooperative Control* pp 310–21

[42] Jiang C, Ni B Y, Han X and Tao Y R 2014 Non-probabilistic convex model process: a new method of time-variant uncertainty analysis and its application to structural dynamic reliability problems *Comput. Methods Appl. Mech. Eng.* **268** 656–76

[43] Jiang C, Ni B Y, Liu N Y, Han X and Liu J 2016 Interval process model and non-random vibration analysis *J. Sound. Vib.* **373** 104–31

[44] Catlin D E 1989 *Estimation, Control, and the Discrete Kalman Filter* (Springer)

[45] Grewal M S and Andrews A P 2014 *Kalman Filtering: Theory and Practice with MATLAB* (Wiley)

[46] Jiang C, Li J W, Ni B Y and Fang T 2019 Some significant improvements for interval process model and non-random vibration analysis method *Comput. Methods Appl. Mech. Eng.* **357** 112565

[47] Resnick S I 2013 *Adventures in Stochastic Processes* (Springer)

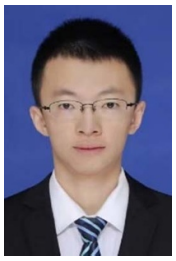
[48] Elishakoff I, Elisseeff P and Glegg S A 1994 Nonprobabilistic, convex-theoretic modeling of scatter in material properties *AIAA J.* **32** 843–9

[49] Wu J L, Zhang Y Q, Chen L P and Luo Z 2013 A Chebyshev interval method for nonlinear dynamic systems under uncertainty *Appl. Math. Model.* **37** 4578–91

[50] Kang Z and Zhang W B 2016 Construction and application of an ellipsoidal convex model using a semi-definite programming formulation from measured data *Comput. Methods Appl. Mech. Eng.* **300** 461–89

[51] Qiu Z P and Wang X J 2003 Comparison of dynamic response of structures with uncertain-but-bounded parameters using

non-probabilistic interval analysis method and probabilistic approach *Int. J. Solids Struct.* **40** 5423–39
[52] Ponce Campuzano J C, Matthews K E and Adams P 2018 On the use of history of mathematics: an introduction to Galileo's study of free fall motion *Int. J. Math. Educ. Sci. Technol.* **49** 517–29
[53] Lin X Y, Luo H Z and Fan W Q 2010 An improved GPS dynamic positioning filtering method *J. Nav. Aer. Eng. Coll.* **25** 361–4
[54] Britting K R 2010 *Inertial Navigation Systems Analysis* (Wiley)
[55] Chang L, Li J and Chen S 2014 Initial alignment by attitude estimation for strapdown inertial navigation systems *IEEE Trans. Instrum. Meas.* **64** 784–94



Jinyang Li, PhD candidate at Hunan University. His research interests include reliability analysis and uncertainty propagation analysis.



Jinwu Li, received his PhD degree in Mechanical Engineering from Hunan University, People's Republic of China, in 2020. His research interests include uncertainty quantification, intelligent design, and reliability design.



Chengkai Shen, received an MS degree in Mechanical Engineering from Hunan University, Changsha, People's Republic of China, in 2022. His research interests include Kalman filter and uncertainty quantification.



Chao Jiang, PhD, is currently a professor at the College of Mechanical and Vehicle Engineering and vice president of Hunan University. His academic research is mainly focused on mechanical design, with particular interests in the scientific issues of uncertainty quantification and analysis, structural reliability, optimization design, and fracture and fatigue.



Bingyu Ni, associate professor, received a PhD degree in Mechanical Engineering from Hunan University in 2017. His main research interests include uncertainty analysis in structural dynamics, spatial uncertainty quantification and propagation, and structural interval finite element analysis, etc.